Polyhedron

Volume 120, 14 December 2016, Pages 18–29

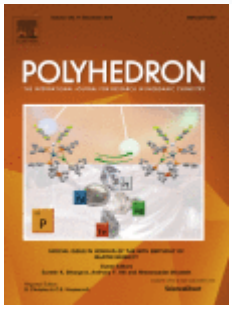

Assembly of high nuclearity clusters from a family of tripodal *tris*-carboxylate ligands

- Stephen P. Argent[a],
- Irina Tarassova[a],
- Alex Greenaway[a],
- Harriot Nowell[b],
- Sarah A. Barnett[b],
- Mark R. Warren[b],
- Chiu C. Tang[b],
- Christopher G. Morris[a, c],
- William Lewis[a],
- Neil R. Champness[a, ·],

Show more

https://doi.org/10.1016/j.poly.2016.04.029

Abstract

A family of four tris-carboxylic acid ligands 1,3,5-tris(4′-carboxybiphenyl-2-yl)benzene (**H_3L^1**), 1,3,5-tris-2-carboxyphenylbenzene (**H_3L^2**), 1,3,5-tris(4″-carboxy-para-terphenyl-2-yl)benzene (**H_3L^3**) and 1,3,5-tris(3′-carboxybiphenyl-2-yl)benzene (**H_3L^4**) have been synthesised and reacted with first row transition metal cations to give nine complexes which have been structurally characterised by X-ray crystallography. The ligands share a common design motif having three arms connected to a benzene core via three *ortho*-disubstituted phenyl linkers. The ligands vary in length and direction of the carboxylic acid functionalised arms and are all able to adopt tripodal conformations in which the three arms are directed facially. The structures of $[Zn_8(\mu_4\text{-}O)(L^1)_4(HCO_2)_2(H_2O)_{0.33}(DMF)_2]$ (**1a-Zn**), $[Co_{14}(L^2)_6((\mu_3\text{-}OH)_8(HCO_2)_2(DMF)_4(H_2O)_6]$ (**2-Co**), $[Ni_{14}(L^2)_6(\mu_3\text{-}OH)_8(HCO_2)_2(DMF)_4(H_2O)_6]$ (**2-Ni**), $[Zn_8(\mu_4\text{-}O)(L^3)_4(DMF)(H_2O)_4(NO_3)_2]$ (**3-Zn**), $[Ni_5(\mu\text{-}OH)_4(L^2)_2(H_2O)_6(DMF)_4]$ (**5-Ni**), $[Co_8(\mu_4\text{-}O)_4(L^4)_4(DMF)_3(H_2O)]$ (**6-Co**) and $Fe_3(\mu_3\text{-}O)(L4)_2(H_2O)(DMF)_2)]$ (**7-Fe**) contain polynuclear clusters surrounded by ligands $(L^{1\text{–}4})^{3-}$ in tripodal conformations. The structure of $[Zn_2(HL^1)_2(DMF)_4]$ (**1b-Zn**) shows it to be a binuclear complex in which the two ligands $(HL^2)^{2-}$ are partially deprotonated whilst $\{[Zn_3(L^2)_2(DMF)(H_2O)(C_5H_5N)]\cdot 6(DMF)\}_n$ (**4-Zn**) is a 2D coordination network containing $\{Zn_2(RCO_2)_4(solv)_2\}$ paddlewheel units. The

conformations of the ligand arms in the complexes have been analysed, confirming that the shared *ortho*-disubstituted phenyl ring motif is a powerful and versatile tool for designing ligands able to form high-nuclearity coordination clusters when reacted with transition metal cations.

Graphical abstract

A family of four tris-carboxylic acid ligands **$H_3L^{1–4}$** have been synthesised and reacted with first row transition metal cations to give nine complexes which have been structurally characterised by X-ray crystallography. The ligands share a common design motif having three arms connected to a benzene core via three *ortho*-disubstituted phenyl linkers and show a propensity to form high nuclearity complexes.

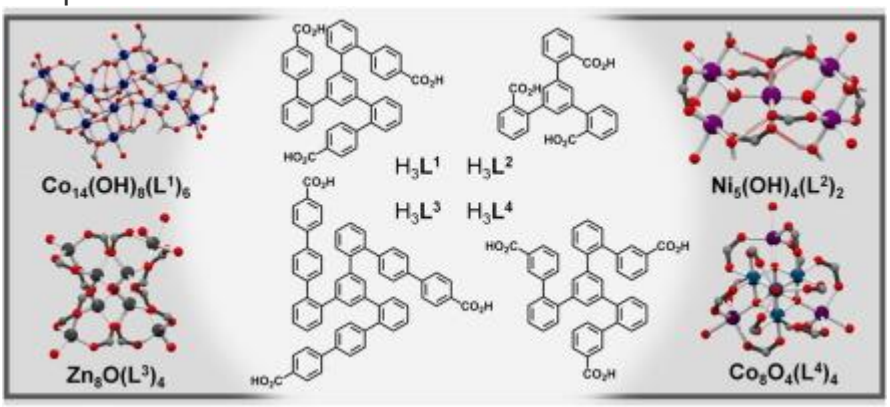

Figure options

Keywords

- High nuclearity cluster;
- Metal-directed assembly;
- Carboxylate bridging;
- Basic carboxylate;
- Crystal structure

1. Introduction

Multi-metallic coordination clusters are of interest from the perspectives of both fundamental [1] and application-targeted [2] chemistry. Examples have been shown to have interesting magnetic properties [3] ; [4], to act as mimics for active sites of enzymes [5] ; [6] or to have utility as structural building units for the design and synthesis of metal–organic frameworks (MOFs) [7]. Strategies used to promote the formation of high-nuclearity complexes include incorporating bulky peripheral groups into ligands in order to restrict the coordination number at metal centres, resulting in the remaining sites being occupied by small hydroxy- and oxo-ligands [8]; [9] ; [10]. An alternative strategy is to use polytopic ligands with closely spaced binding domains able to span multiple metal cations. A ligand in which the binding domains are rigidly pre-organised will help to overcome the entropic penalty associated with forming the high degree of order typical of polynuclear clusters [11]; [12] ; [13].

We have previously used polytopic carboxylate ligands with aromatic spacers as linkers for the synthesis of a wide variety of porous MOFs with applications in gas storage and separation [14]; [15]; [16] ; [17]. The formation of MOFs requires ligands with divergent binding domains which lead to poly-dimensional networks. We argued that the same chemical design elements could be used to synthesise ligands with convergent binding domains which would fulfil the requirements of a 'pre-organisation' strategy. We have reported the tripodal ligand 1,3,5-tris(4′-carboxybiphenyl-2-yl)benzene $\mathbf{H_3L^1}$ which binds Cd(II) cations to form a large polynuclear nano-sphere complex $[Cd_{66}(\mu_3\text{-}OH)_{28}(\mu_3\text{-}O)_{16}(\mu_5\text{-}NO_3)_{12}(\mathbf{L^1})_{20}(\mu_2\text{-}DMF)_{12}\subset(DMF)_9]$ with an unprecedented metallo-ligand core–shell structure [18]. This threefold symmetric ligand features three *ortho*-diphenylbenzene motifs which can orient the three carboxylic acid binding domains either all to the same face of the ligand (*endo* conformation) or one above and two below the plane of the ligand (*exo* conformation). Both of these conformations were observed in the reported family of complexes of $(L^1)^{3-}$ with Cd(II) cations. When the ligand adopts an *endo* conformation the ligand can exhibit a propeller-like twist in its three arms giving it chiral C_3 symmetry. The pitch of this propeller twist varies and dictates the distance *d*between the pendant carboxylate groups (Scheme 1). The degree of twist can be defined by the torsion angles ϕ^1 along the bonds between the central phenyl ring and three *ortho*-disubstituted phenyl rings [19]. A second torsion angle ϕ^2 between the *ortho*-disubstituted phenyl rings and carboxylic acid functionalised phenyl rings does not alter the distance *d* between the three carboxylate groups, but it does influence their orientations.

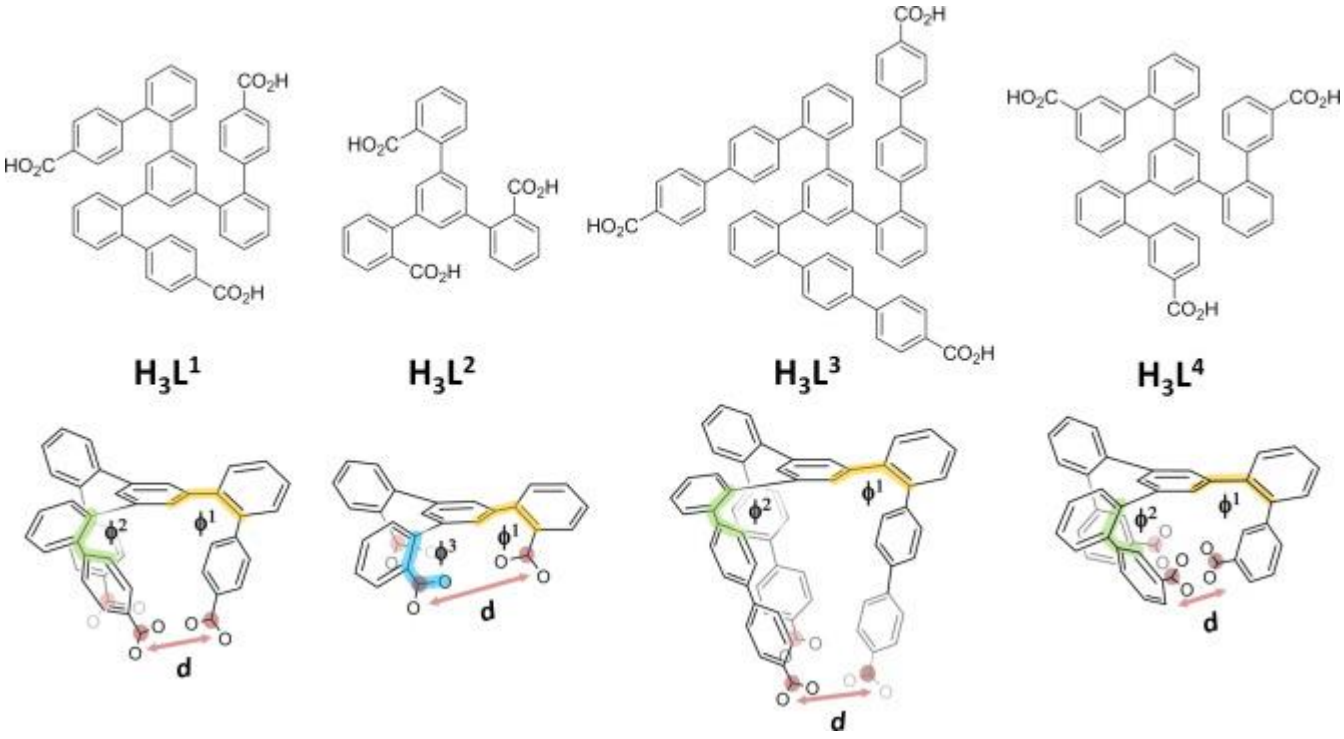

Scheme 1.

View of $\mathbf{H_3L^{1–4}}$ with representations of their tripodal *endo* conformations highlighting key torsion angles ϕ^1, ϕ^2 and ϕ^3 and intraligand carboxylate separation distance *d*.

Figure options

We report herein a family of tris-carboxylic acid ligands $\mathbf{H_3L^{1–4}}$ and their reactions with a variety of first-row transition metal cations to explore the propensity of these

tripodal ligands to form polynuclear clusters. The ligands **$H_3L^{1–4}$** share the central design principle in having three arms with pendant carboxylic acid moieties attached to a central benzene ring *via ortho*-substituted phenyl linkages. The new ligands differ from **H_3L^1** in three ways: decreasing or increasing the length of the spacers in the three arms of the ligand (**H_3L^2** and **H_3L^3**, respectively) or changing the location of the phenylcarboxylic acid group from the *para* to the *meta* positions of the linkages (**H_3L^4**). The resulting array of one two-dimensional network and eight discrete complexes exhibits a variety of ligand conformations, ancillary co-ligands and metal-coordination motifs.

2. Experimental

2.1. Synthesis

H_3L^1 was synthesised according to our previously described method [18]. We report an improved synthesis of the previously reported [20] ligand 1,3,5-tris-2-carboxyphenylbenzene **H_3L^2**. 4-(Ethoxycarbonyl)phenylboronic acid **12** and 3-(ethoxycarbonyl)phenylboronic acid **18** were purchased from Frontier Scientific. Bromo-1-(2,3-dihydro-1*H*-naphtho[1,8-*de*]-1,3,2-diazaborinyl)benzene **11** was synthesised starting from 4-bromophenylboronic acid **10** according to a literature method [21]. 1,3,5-Tris(2-bromophenyl)benzene **15** was synthesised from 2′-bromoacetophenone **16**according to a literature method [22]. ^{1}H NMR and ^{13}C NMR spectra were measured on Bruker DPX400, AV400 and AV(III)400 spectrometers. High-resolution electrospray mass spectra were measured on a Bruker MicroTOF spectrometer. MALDI-TOF mass spectra were measured using a Bruker Spectroflex III mass spectrometer with DCTB (*trans*-2-[3-(4-*tert*-butylphenyl)-2-methyl-2-propenylidene]malononitrile) as a matrix. Where yields for complexation reactions have been given they are calculated based on the mass of the solvated material as indicated by interpretation of elemental analysis.

2.1.1. 1,3,5-Tris-2-methylphenylbenzene (9)

2′-Methylacetophenone **8** (20.0 g, 150.0 mmol) and trifluoromethanesulfonic acid (2.50 g, 15.0 mmol) were added cautiously to a round-bottom flask before being stirred and heated at 130 °C under N_2 for 24 h. During the course of the reaction a viscous black mixture formed which solidified upon cooling to room temperature. The crude reaction mixture was quenched by addition of water (5 cm^3) before being extracted with dichloromethane which was washed with water and brine, dried over $MgSO_4$ and concentrated under reduced pressure. The resulting crude product was recrystallised from chloroform and methanol giving **9** as a colourless crystalline solid (yield 16.0 g, 89%). ^{1}H NMR (CD_2Cl_2, 400 MHz) δ 7.24–7.35 (m, 15H), 2.40 (s, 9H). ^{13}C NMR ($CDCl_3$, 400 MHz) δ 141.1, 140.9, 134.9, 130.0, 129.5, 128.1, 126.9, 125.4, 21.1. ESI-TOF-HRMS: *m*/*z* Calc. for $C_{27}H_{24}$: 348.1878. Found 348.1882 [M]$^+$. Elemental *Anal.* Calc. for $C_{27}H_{24}$: C, 93.06; H, 6.94. Found: C, 92.89; H, 6.87%. ATR-FTIR (cm^{-1}): 3019 (w), 1423(m), 1389(w), 1216(m), 1110(s), 754(s), 669(s).

2.1.2. 1,3,5-Tris-2-carboxyphenylbenzene ($H_3L^2 \cdot 3(H_2O)$)

$KMnO_4$ (8.00 g, 50.6 mmol) was added portion-wise over 5 days to a stirred solution of 1,3,5-tris-2-methylphenylbenzene **9** (2.10 g, 6.0 mmol) and NaOH (2.10 g, 52.5 mmol) in a mixture of water (60 cm^3) and *tert*-butanol (60 cm^3), with the temperature maintained at 55 °C. The mixture was then heated at 80 °C for 1 h before the hot mixture was filtered and the filtrate concentrated under reduced pressure. The solution was acidified with concentrated HCl (10 cm^3) resulting in precipitation of **H_3L^2** as a white solid which was collected, washed with water and

dried *in vacuo* (yield 1.30 g, 60%). ^{1}H NMR ($CDCl_3$, 400 MHz) δ 7.94 (dd, J = 7.6, 1.0 Hz, 3H), 7.53 (td, J = 7.6, 1.2 Hz, 3H), 7.40 (td, J = 7.2, 1.2 Hz, 3H), 7.34 (dd, J = 7.2, 1.0 Hz, 3H), 7.18 (s, 3H). ESI-TOF-HRMS: m/z Calc. for $C_{27}H_{18}O_{18}Na$: 461.001. Found 461.1004 $[M+Na]^+$. Elemental *Anal.* Calc. for $C_{27}H_{18}O_{18}\cdot(H_2O)_3$: C, 65.85; H, 4.91. Found: C, 65.50; H, 4.57%. ATR-FTIR (cm^{-1}): 3444 (br), 2790 (m, br), 2490 (m, br), 1680 (s), 1422(s), 1260 (s), 1070 (m), 754 (m), 669(m).

2.1.3. Ethyl-4'-(1H-naphtho[1,8-de][1,3,2]diazaborinin-2(3H)-yl)-[1,1'-biphenyl]-4-carboxylate (13)

Bromo-1-(2,3-dihydro-1*H*-naphtho[1,8-*de*]-1,3,2-diazaborinyl)benzene **11** (2.40 g, 7.43 mmol), 4-(ethoxycarbonyl)phenylboronic acid **12** (2.40 g, 12.4 mmol), powdered tripotassium phosphate (3.40 g, 20.7 mmol) and 1,4-dioxane (150 cm^3) were added to a round-bottom flask fitted with a condenser and heated at 80 °C for 15 min under N_2. $Pd(PPh_3)_4$ (0.47 g, 0.41 mmol) was added to the mixture which was purged with N_2 for a further 15 min before being stirred at 80 °C for 2 days. The mixture was allowed to cool, filtered and the filtrate concentrated under reduced pressure. The resulting residue was dissolved in chloroform (100 cm^3), washed with water (3 × 50 cm^3) and brine (50 cm^3) and concentrated under reduced pressure to give a brown solid, which was recrystallised from chloroform and methanol to give **13** as large yellow needles (yield 2.07 g, 71%). ^{1}H NMR ($CDCl_3$, 400 MHz) δ 8.25–8.04 (m, 2H), 7.85–7.67 (m, 6 H), 7.19 (dd, J = 7.3, 8.2 Hz, 2H), 7.11 (d, J = 7.8 Hz, 2H), 6.48 (dd, J = 0.8, 7.3 Hz, 2H), 6.11 (s, 2 H), 4.45 (q, J = 7.2 Hz, 2H), 1.46 (t, J = 7.2 Hz, 3H). ESI-TOF-MS: m/z 392.23 $[M]^+$. Elemental *Anal.*Calc. for $C_{25}H_{21}BN_2O_2$: C, 76.55; H, 5.40; N, 7.14. Found: C, 76.51; H, 5.33; N, 7.26%. ATR-FTIR (cm^{-1}): 3360 (s), 2900 (m), 1590 (s), 1580 (s), 1360 (m), 1260 (s), 1080 (m), 756 (m, br), 728 (m).

2.1.4. (4'-(Ethoxycarbonyl)-[1,1'-biphenyl]-4-yl)boronic acid (14)

To a stirred solution of ethyl-4′-(1*H*-naphtho[1,8-*de*][1,3,2]diazaborinin-2(3*H*)-yl)-[1,1′-biphenyl]-4-carboxylate **13** (1.00 g, 2.50 mmol) in THF (80 cm^3) was added H_2SO_4 (2 M, 12.8 cm^3) and the solution stirred overnight at room temperature resulting in formation of a white precipitate. The solid was removed by filtration and the filtrate was diluted with ethyl acetate (30 cm^3) and washed sequentially with water (4 × 50 cm^3) and brine (2 × 25 cm^3), dried over $MgSO_4$, concentrated under reduced pressure and triturated with pentane to give **14** as a pale yellow powder (yield 0.541 g, 92%). ^{1}H NMR ($CDCl_3$, 400 MHz) δ 8.82–8.66 (m, 2H), 8.59 (d, J = 1.5 Hz, 2H), 8.43 (d, J = 8.2 Hz, 2H), 7.96–7.81 (m, 2H), 4.60–4.40 (m, 2H), 1.53–1.41 (m, 3H). ESI-TOF-HRMS: m/z Calc. for $C_{15}H_{16}BO_4$: 271.1142. Found 271.1032 $[M + H]^+$. Elemental *Anal.* Calc. for $C_{15}H_{15}BO_4$: C, 66.70; H, 5.60. Found: C, 66.65; H, 5.43%. ATR-FTIR (cm^{-1}): 3330 (s, br), 2980 (m), 1710 (s), 1600 (s), 1270 (s, br), 1100 (s), 1000 (m), 735 (m), 722 (m).

2.1.5. 1,3,5-Tris(4"(ethoxycarbonyl)-para-terphenyl-2-yl)benzene chloroform solvate ($Et_3L^3\cdot CHCl_3$)

1,3,5-Tris-2′-bromophenylbenzene **15** (168 mg, 0.309 mmol), (4′-(ethoxycarbonyl)-[1,1′-biphenyl]-4-yl)boronic acid **14** (500 mg, 1.85 mmol), CsF (565 mg, 3.72 mmol) and tris(dibenzylideneacetone)dipalladium(0) $[Pd_2(DBA)_3]$ were added to 1,4-dioxane (25 cm^3) and heated at 80 °C under N_2 for 15 min. Tri-*tert*-butylphosphine (25.0 mg, 0.124 mmol) was added and the reaction mixture stirred at 80 °C for 18 h before being allowed to cool. The solid residue was removed by centrifugation and the resultant solution concentrated under reduced pressure. The resulting residue was dissolved in toluene (20 cm^3), washed with water (4 × 20 cm^3), brine (2 × 20 cm^3), dried over $MgSO_4$and concentrated under reduced pressure resulting in a grey solid, which was recrystallised from chloroform and methanol to give **$Et_3L^3\cdot CHCl_3$** as white

crystals (yield 150 mg, 44%). ^{1}H NMR ($CDCl_3$, 400 MHz) δ 8.12 (d, J = 8.3 Hz, 6H), 7.48–7.32 (m, 15H), 7.31–7.17 (m, 6H), 7.08–6.92 (m, 9 H), 6.82 (s, 3H), 4.47 (d, J = 7.0 Hz, 6H), 1.48 (t, J = 7.2 Hz, 9H). ESI-TOF-MS: m/z 1001.2 $[M+Na]^+$. Elemental *Anal.* Calc. for $C_{69}H_{54}O_6 \cdot CHCl_3$: C, 76.53; H, 5.05. Found: C, 76.65; H, 4.66%.

2.1.6. 1,3,5-Tris(4"carboxy-para-terphenyl-2-yl)benzene (H$_3$L^3)

To a stirred suspension of **Et$_3$L^3·CHCl$_3$** (100 mg, 0.0912 mmol) in 2-propanol (20 cm^3) was added saturated aqueous KOH (1 cm^3). The mixture was heated under reflux for 8 h resulting in dissolution of all the material. The volume of solvent was reduced to 10 cm^{3}under reduced pressure before the solution was acidified with concentrated hydrochloric acid (5 cm^3) resulting in formation of a white precipitate, which was collected and washed sequentially with water, methanol and diethyl ether to give **H$_3$L^3** as a white solid (yield 51 mg, 62%). ^{1}H NMR (DMSO-d_6, 400 MHz) δ 8.02 (d, J = 8.4 Hz, 6H), 7.48–7.40 (m, 15H), 7.40–7.32 (m, 6H), 7.28 (t, J = 7.4 Hz, 3H), 7.01 (d, J = 7.5 Hz, 3H), 6.92 (d, J = 7.8 Hz, 6H), 6.72 (s, 3H). MALDI-TOF-MS: m/z 917.4 $[M + Na]^+$. Elemental *Anal.* calc. for $C_{63}H_{42}O_6$: C, 84.54; H, 4.73. Found: C, 83.12; H, 4.36%. ATR-FTIR (cm^{-1}): 3260 (br), 1670 (s), 1600 (m), 1320 (w), 1030 (s, br), 755 (s).

2.1.7. 1,3,5-Tris(3'(ethoxycarbonyl)biphenyl-2-yl)benzene (Et$_3$L^4)

1,3,5-Tris-2′-bromophenylbenzene **15** (500 mg, 0.921 mmol), 3-(ethoxycarbonyl)phenylboronic acid **18** (894 mg, 4.61 mmol), K_2CO_3 (1.15 g, 8.30 mmol) and $Pd(PPh_3)_4$ (29 mg, 0.0249 mmol) were added to a mixture of toluene (90 cm^3), ethanol (10 cm^3) and water (10 cm^3) which was then heated at 70 °C and purged with $N_2$for 15 min. The reaction mixture was stirred at 70 °C for 2 days before being allowed to cool. The reaction mixture was filtered, and water (50 cm^3) was added to the filtrate which was extracted into toluene. The toluene extract was then washed with water (4 × 30 cm^3) and brine (2 × 30 cm^3), dried over $MgSO_4$ and concentrated under reduced pressure to give an orange oil which was purified by column chromatography (15% ethyl acetate in hexane on silica) to give **Et$_3$L^4** as a white solid (yield 387 mg, 56%). ^{1}H NMR ($CDCl_3$, 400 MHz) δ 8.04 (t, J = 1.5 Hz, 3H), 7.89 (dt, J = 7.7, 1.3 Hz, 3H), 7.27–7.43 (m, 12H), 7.00 (dt, J = 7.8, 1.3 Hz, 3H), 6.8 (d, J = 7.4 Hz, 3H), 7.76 (s, 3H), 4.39 (q, J = 7.1, 6H), 1.39 (t, J = 7.1, 9H). ESI-TOF-HRMS: m/z Calc. for $C_{51}H_{42}O_6Na$: 773.2879. Found 773.2771 $[M+Na]^+$. Elemental *Anal.* Calc. for $C_{51}H_{42}O_6$: C, 81.58; H, 5.64. Found: C, 81.50; H, 5.22%.

2.1.8. 1,3,5-Tris(3'-carboxybiphenyl-2-yl)benzene (H$_3$L^4)

The same synthetic method as for **H$_3$L^3** was used to give **H$_3$L^4** as a white solid. ^{1}H NMR (DMSO-d_6, 400 MHz) δ 7.88 (d, J = 7.53 Hz, 3H), 7.81 (s, 3H), 7.47 (t, J = 7.72 Hz, 3H), 7.38–7.43 (m, 3H), 7.30 (t, J = 6.53 Hz, 3H), 7.06 (d, J = 7.40 Hz, 3H), 6.77 (d, J = 7.40 Hz, 3H), 6.66 (s, 3H). ES-TOF-MS: m/z 689.7 $[M + Na]^+$. Elemental *Anal.* calc. for $C_{45}H_{30}O_6$: C, 81.07; H, 4.54. Found: C, 82.01; H, 4.89%.

2.1.9. [Zn$_8$(μ$_4$-O)(L^1)$_4$(HCO$_2$)$_2$(H$_2$O)$_{0.33}$(DMF)$_2$]·7.75(DMF) (1a-Zn)

H$_3$L^1 (20 mg, 0.030 mmol) and $Zn(NO_3)_2 \cdot 6H_2O$ (71 mg, 0.240 mmol) were dissolved in DMF (3 cm^3) and heated in a sealed vial at 85 °C for 3 days resulting in formation of large colourless crystals with the shape of Clovis points [23]. Single crystals for X-ray analysis were taken directly from the mother liquor. The bulk sample was washed with fresh DMF, collected by filtration and dried *in vacuo* to give **1a-Zn**·2(DMF) as a white solid (yield 7 mg, 26%). Upon standing in the cooled DMF reaction mixture for more than 5 days the crystals were observed to re-dissolve. ^{1}H NMR ($CDCl_3$, 400 MHz) δ 8.22 (d-br, J = 7.8 Hz, 12H), 8.05 (s-br, 48H, DMF), 7.75

(d-br, *J* = 7.40 Hz, 12H), 7.24–7.43 (m, 48H), 7.18 (d, *J* = 7.2 Hz, 12H), 6.67 (s, 12H), 5.69 (d-br, *J* = 8.3 Hz, 12H), 2.99 (s, 36H, DMF), 2.92(s, 36H, DMF). MALDI-TOF-MS: *m*/*z* Calc. for $Zn_8O(C_{45}H_{27}O_6)_4(HCO_2)(H_2O)$: 3243.2.* Found 3261.8 [M-HCO_2-(solv)]$^+$. Elemental *Anal.* Calc. for $Zn_8O(C_{45}H_{27}O_6)_4(HCO)_2(C_3H_7NO)_8$: C, 63.95; H, 4.32; N, 2.90. Found: C, 63.80; H, 3.73; N, 2.27%. **Most abundant peak in simulated isotopic distribution at m/z 3258.2.*

2.1.10. [Zn_2(HL^1)$_2$(DMF)$_4$]·2(DMF) (1b-Zn)

H_3L^1 (10 mg, 0.0150 mmol) and $Zn(NO_3)_2·6H_2O$ (27 mg, 0.090 mmol) were dissolved in DMF (1 cm^3) into which was diffused diisopropyl ether resulting in formation of large colourless crystal plates amongst amorphous white materials. Single crystals were taken directly from the mother liquor for X-ray analysis.

2.1.11. [Co_{14}($L2$)$_6$((μ_3-OH)$_8$(HCO_2)$_2$(DMF)$_4$(H_2O)$_6$]·28(DMF) (2-Co)

H_3L^1 (20 mg, 0.030 mmol) and $Co(NO_3)_2·6H_2O$ (69 mg, 0.240 mmol) were dissolved in DMF (3 cm^3) and heated in a sealed vial at 85 °C for 5 days resulting in formation of pink rhombic crystal plates. Crystals for single crystal X-ray analysis were taken directly from the mother liquor. The bulk sample was washed with fresh DMF, collected by filtration, washed with diethyl ether and dried *in vacuo* to give **2-Co**·8(DMF) as a pink solid (yield 19 mg, 11%). Elemental *Anal.* Calc. for $Co_{14}(OH)_8(C_{45}H_{27}O_6)_6(HCO_2)_2(H_2O)_6(C_3H_7NO)_4·8(C_3H_7NO)$: C, 61.47; H, 4.49; N, 2.79. Found: C, 62.15; H, 4.03; N, 2.58%.

2.1.12. [Ni_{14}($L2$)$_6$(μ_3-OH)$_8$(HCO_2)$_2$(DMF)$_4$(H_2O)$_6$]·24(DMF) (2-Ni)

The same synthetic method was used as for **2-Co**. **H_3L^1** (20 mg, 0.030 mmol) and $Ni(NO_3)_2·6H_2O$ (70 mg, 0.240 mmol). After 5 days heating small green rhombic crystal plates were observed amongst pale green amorphous material. Single crystals were manually selected for X-ray analysis. Satisfactory analytical results for the bulk material could not be obtained.

2.1.13. [Zn_8(μ_4-O)(L^3)$_4$(DMF)(H_2O)$_4$](NO_3)$_2$·16(DMF) (3-Zn)

The same synthetic method was used as for **1a-Zn**, using **H_3L^3** (10 mg, 0.0112 mmol), $Zn(NO_3)_2·6H_2O$ (16 mg, 0.0559 mmol) and DMF (1.5 cm^3). After 2 days colourless hexagonal plate crystals (yield 18 mg) were obtained. Elemental *Anal.* Calc. for $Zn_8O(C_{63}H_{42}O_6)_4(NO_3)_2(H_2O)_6(C_3H_7NO)_{10}$*: C, 66.65; H, 4.96; N, 3.31. Found: C, 63.20; H, 5.61; N, 3.14%. **Closest plausible match to the obtained analysis; the analysis is likely to be affected by ambiguity in the identity of the coordinated counter ion.*

2.1.14. {[Zn_3(L^2)$_2$(DMF)(H_2O)(C_5H_5N)]·6(DMF)}$_n$ (4-Zn)

The same synthetic method was used as for **1a-Zn** using **H_3L^2·3(H_2O)** (20 mg, 0.0407 mmol) and $Zn(NO_3)_2·6H_2O$ (59 mg, 0.203 mmol) in DMF (3 cm^3) and pyridine (0.1 cm^3) resulting in formation of colourless blocky crystals (yield 36 mg, 58%). Elemental *Anal.* Calc. for $Zn_3(C_{27}H_{18}O_6)_2(H_2O)_6(C_5H_5N)(C_3H_7NO)_{3.5}$: C, 55.06; H, 5.12; N, 4.16. Found: C, 55.43; H, 5.35; N, 3.92%.

2.1.15. [Ni_5(μ-OH)$_4$(L^2)$_2$(H_2O)$_6$(DMF)$_4$]·6(DMF) (5-Ni)

H_3L^2·3(H_2O) (10 mg, 0.0203 mmol) and $Ni(NO_3)_2·6H_2O$ (30 mg, 0.102 mmol) were dissolved in DMF (1.4 cm^3) and heated in a sealed vial at 80 °C for 5 days. Diisopropyl ether vapour was diffused into the resultant green solution resulting in the formation of a small number of green blocky crystals, which were taken directly from the mother liquor for single crystal X-ray analysis.

2.1.16. [Co_8(μ_4 -O)$_4$($L4$)$_4$(DMF)$_3$(H_2O)]·3(H_2O)·6(DMF) (6-Co)

H_3L^4 (20 mg, 0.030 mmol) and $Co(NO_3)_2·6H_2O$ (44 mg, 0.150 mmol) were dissolved in DMF (2 cm^3) and heated in a sealed vial at 80 °C for 2 days resulting in formation of small black block crystals. Crystals were either taken directly from the mother

liquor for single crystal X-ray analysis or washed with fresh DMF, collected by filtration and dried *in vacuo*to give **6-Co**·4(DMF) as a black solid (yield 27 mg, 24%). Elemental *Anal.* Calc. for $Co_8O_4(C_{27}H_{18}O_6)_4(C_3H_7NO)_4(H_2O)_{15}$: C, 50.72; H, 4.33; N, 2.40. Found: C, 51.02; H, 3.60; N, 3.88%.

2.1.17. [Fe_3 (μ^3-O)($L4)_2(H_2O)(DMF)_2$)]·10(DMF) (7-Fe)

H_3L^4 (20 mg, 0.030 mmol) and $Fe(NO_3)_3{\cdot}nH_2O$ (45 mg) were dissolved in DMF (2 cm^3) and heated in a sealed vial at 80 °C for 2 days resulting in formation of very small brown lath-shaped crystals amongst amorphous brown material. Crystals were taken directly from the mother liquor for single crystal X-ray analysis.

2.2.1. Single crystal X-ray diffraction studies

Crystals were mounted under a film of Fomblin perfluoropolyether on a Mitegen Micromount and flash-frozen under a cold stream of N_2. Diffraction data for **1a-Zn**, **1b-Zn**, **2-Co**, **2-Ni**, **3-Zn**, and **6-Co** were collected on a Rigaku Oxford Diffraction SuperNova diffractometer equipped with an Atlas detector and microfocus Cu source. The raw data were reduced and corrected for Lorentz and polarisation effects using CrysAlisPro [24]; corrections for the effects of adsorption were applied using a numerical absorption correction based on Gaussian integration over a multifaceted crystal model. The diffraction data for **4-Zn**, **5-Ni** and **7-Fe** were collected at Diamond Light Source, Beamline I19, on a CrystalLogic Kappa 4-circle diffractometer equipped with a Rigaku Saturn 724 + CCD detector using synchrotron radiation with a wavelength of 0.6889 Å [25]. The raw data were reduced and corrected for Lorentz and polarisation effects using CrystalClear [26] and corrected for the effects of adsorption using Scale implemented in CrystalClear. The structures were solved by direct methods and refined by full-matrix least-squares using the SHELXTL software package [27]. Details of the crystal structure refinements can be found in the Supplementary information.

2.2.2. Powder X-ray diffraction

A dried sample of **6-Co** was lightly ground before being loaded into a 0.5 mm borosilicate capillary. High-resolution powder diffraction data were collected at Diamond Light Source, Beamline I11 using multi-analysing-crystal detectors (MACs) using radiation with a wavelength of 0.826161 Å with the sample maintained at a temperature of 273 K. A Pawley refinement [28] of the data was performed using TOPAS-Academic [29] to extract the unit cell parameters.

3. Results and discussion

3.1. Ligand synthesis

Ligands H_3L^1, H_3L^3 and H_3L^4 were all synthesised using Pd-catalysed Suzuki cross-coupling reactions from the common starting material 1,3,5-tris(2-bromophenyl)benzene **15** which itself was synthesised in good yield from the cyclotrimerization of 2′-bromoacetophenone **16** (Scheme 2). The triple cross-coupling reactions involving this sterically-demanding substrate give at best moderate yields with partially-reacted dehalogenated products accounting for the remaining material. The extended biphenylboronic acid intermediate **14** required to synthesise H_3L^3 was obtained by masking the boronic acid functionality of 4-bromophenylboronic acid **10** using 1,8-diaminonaphthalene [21] before cross-coupling the resulting fragment **11** with 4-(ethoxycarbonyl)phenylboronic acid **12** to

give **13**. The 1,8-diaminonaphthalene protecting group was subsequently removed by acid hydrolysis to reveal the boronic acid functional group. After purification, the triethyl-esters of ligands $\mathbf{H_3L^1}$, $\mathbf{H_3L^3}$ and $\mathbf{H_3L^4}$were hydrolysed with KOH, followed by an acidic work up to give the tris-carboxylic acids. Ligand $\mathbf{H_3L^2}$ was synthesised by the threefold oxidation of the methylphenyl functional groups of 1,3,5-tris-2-methylphenylbenzene **9**, which was synthesised from 2′-methylacetophenone **8** using cyclotrimerization conditions analogous to those used to obtain **15**.

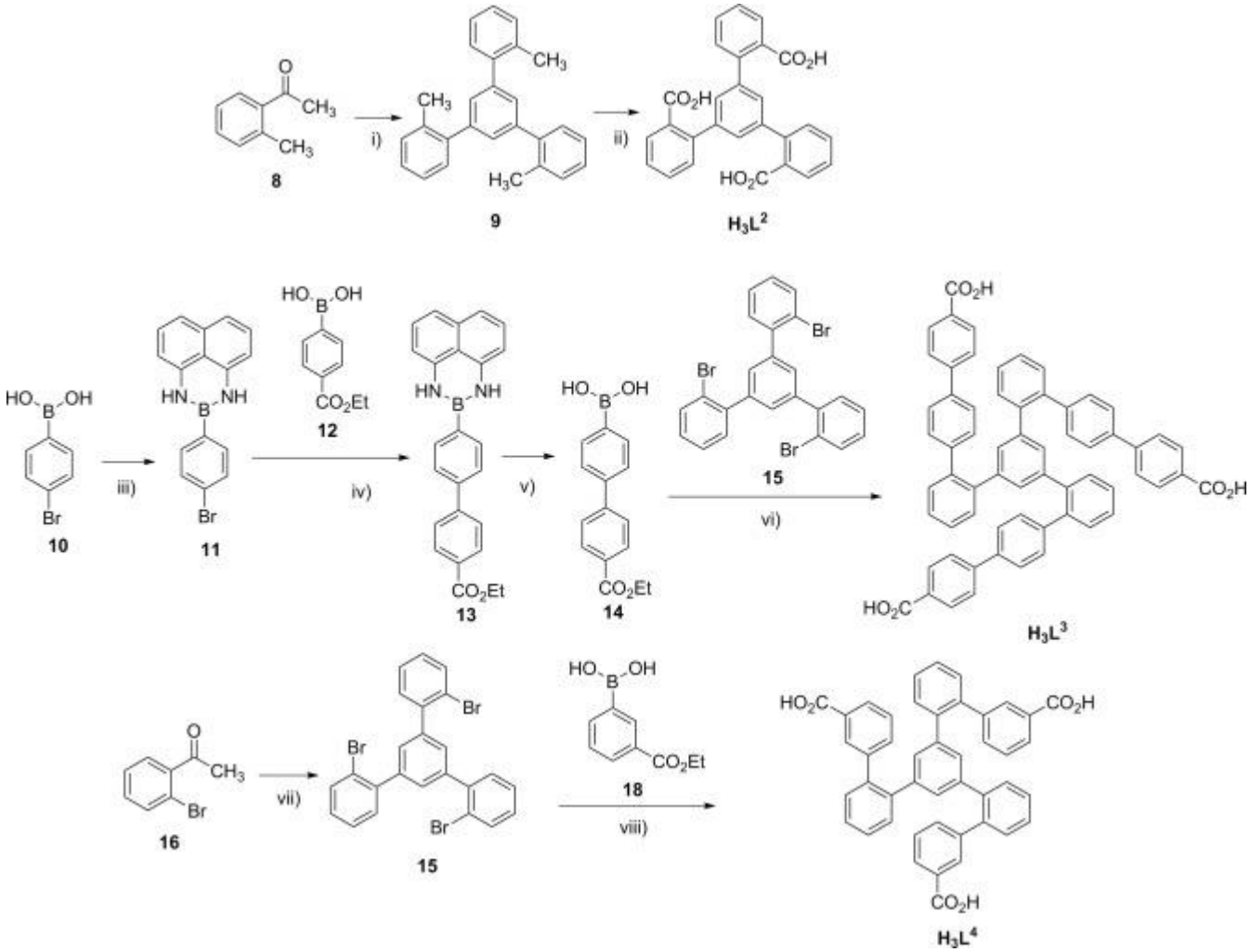

Scheme 2.

Synthesis of $\mathbf{H_3L^{2-4}}$. Conditions: (i) CF_3SO_3H; (ii) $KMnO_4$, KOH; H_2O, ^{t}BuOH (iii) 1,8-diaminonaphthalene, toluene; (iv) $Pd(PPh_3)_4$, K_3PO_4, 1,4-dioxane; (v) H_2SO_4, THF; (vi) (a) $Pd_2(DBA)_3{\cdot}CHCl_3$, CsF, 1,4-dioxane (b) KOH(aq), 2-propanol; (vii) CF_3SO_3H; (viii) (a) $Pd(PPh_3)_4$, K_2CO_3, toluene, EtOH, H_2O, (b) KOH(aq), 2-propanol.

Figure options

3.2. Synthesis, structure and characterisation of complexes of ligands $\mathbf{H_3L^{1-4}}$

3.2.1. $[Zn_8(\mu_4\text{-}O)(L^1)_4(HCO_2)_2(H_2O)_{0.33}(DMF)_2]{\cdot}7.75(DMF)$ (1a-Zn)

Reaction of $\mathbf{H_3L^1}$ with $Zn(NO_3)_2{\cdot}6H_2O$ in DMF for 5 days at 85 °C resulted in formation of a crop of large colourless crystals which X-ray analysis showed to be $[Zn_8(\mu_4\text{-}O)(L^1)_4(HCO_2)_2(H_2O)_{0.33}(DMF)_2]{\cdot}7.75(DMF)$ (**1a-Zn**). The polynuclear cluster crystallises in the centrosymmetric tetragonal space group *I*4$_1$/*a* with one complete complex in the asymmetric unit. Four three-blade paddlewheel SBUs

{$Zn_2(RCO_2)_3$} [30] surround a μ_4-oxo anion which is coordinated to the axial position of the central Zn(II) centre from each paddlewheel (Fig. 1). Four ligands $(L^1)^{3-}$ each in a tripodal *endo* conformation straddle the four faces of the tetrahedral array of SBUs with each of their carboxylate functional groups bound to a different paddlewheel. The outer axial coordination sites on Zn(II) within the four paddlewheels are bound by a disordered mixture of water, DMF and formate ligands and have coordination numbers of either four or five. The central $[Zn_8O(L^1)_4]$ unit has a residual +2 charge which is balanced by the coordinated formate anions resulting from decomposition of DMF during the reaction; both anions are crystallographically modelled at partial occupancies with the remainder of the charge likely balanced by unidentified disordered components. Disregarding ligation by the latter, each $[Zn_8O(L^1)_4]$ unit has distorted tetrahedral symmetry and is chiral as a result of all four tripodal ligands being twisted in the same direction; as the space group is centrosymmetric, complexes of both handedness occur in the unit cell in a 1:1 ratio.

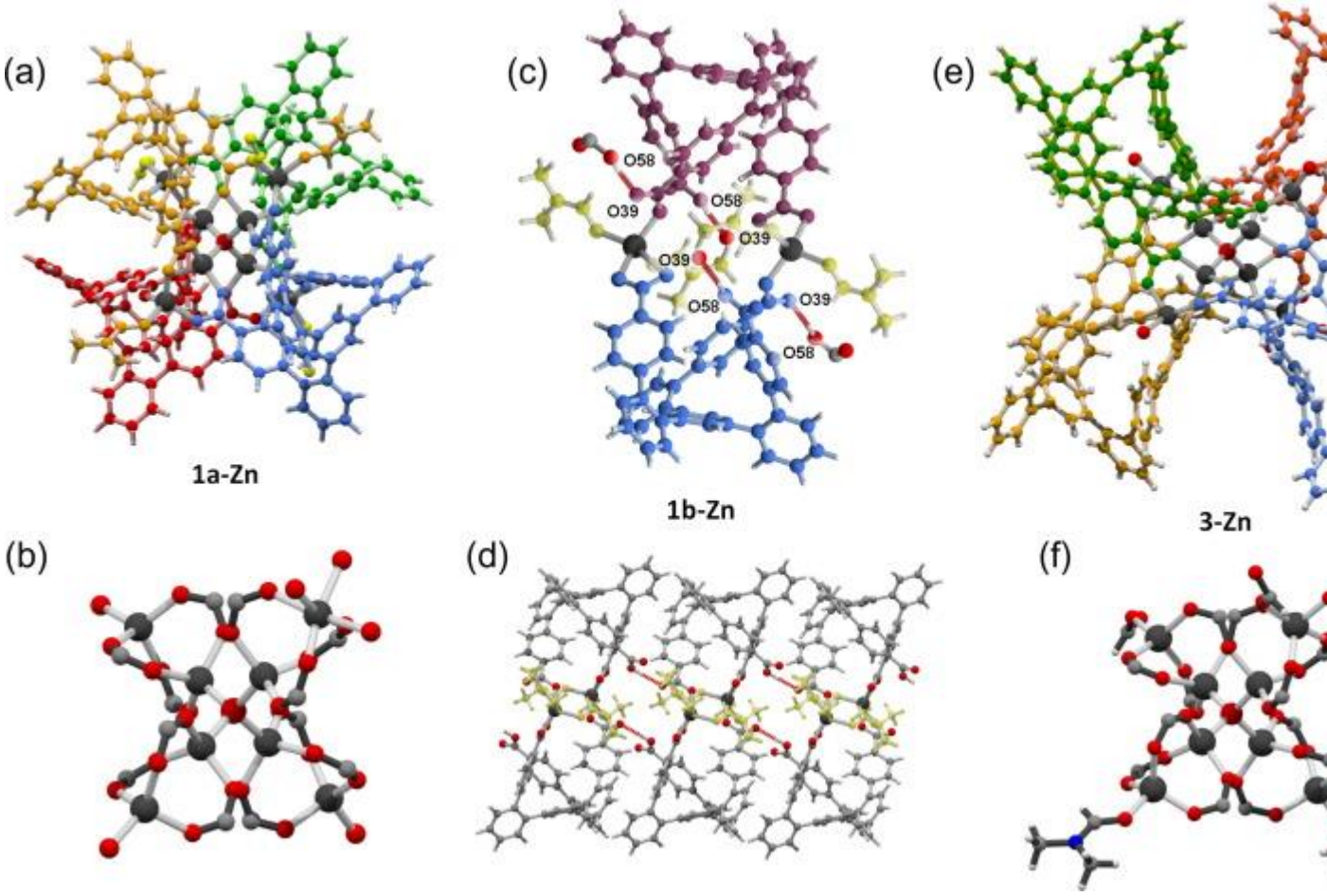

Fig. 1.

View of (a) overall structure and of (b) $Zn_8O(RCO_2)_4$ core in $[Zn_8(\mu_4\text{-}O)(\mathbf{L}^1)_4(HCO_2)_2(H_2O)_{0.33}(DMF)_2]$ (**1a-Zn**): ligands $(L^1)^{3-}$ orange, green, red, blue; DMF orange; formate yellow; zinc black. View of (c) overall structure and of (d) packing of $[Zn_2(\mathbf{HL}^1)_2(DMF)_4]$ (**1b-Zn**): ligands $(L^1)^{3-}$ purple, blue; DMF yellow; zinc black; hydrogen bonds highlighted in red. View of (e) overall structure and of (f) $Zn_8O(RCO_2)_4$ core in $[Zn_8(\mu_4\text{-}O)(\mathbf{L}^3)_4(DMF)(H_2O)_4](NO_3)_2$ (**3-Zn**): colours as for (a). (Color online.)

Figure options

A ^{1}H NMR spectrum of **1a-Zn** dissolved in $CDCl_3$ was measured in order to probe the behaviour of the complex in solution. Six peaks observed between 5.7 and 8.2 ppm

are shifted from the original peak positions observed for free **H_3L^1** in d_6-DMSO and are consistent with the retention of C_3 symmetry in the ligand environment (Fig. S1). A MALDI mass spectrum of **1a-Zn** deposited from an acetonitrile solution contains a broad peak at *m*/*z* of 3261.8 which is assigned as $[Zn_8O(L^1)_4(HCO_2)(H_2O)]^+$ alongside a weaker unassigned peak at a higher *m*/*z* 3878.5 and several peaks at lower *m*/*z* (Fig. S3).

3.2.2. $[Zn_2(HL^1)_2(DMF)_4]\cdot 2(DMF)$ (1b-Zn)

The role of heating in the formation of **1a-Zn** was investigated by diffusing diisopropyl ether into a fresh solution of **H_3L^1** and $Zn(NO_3)_2\cdot 6H_2O$ at room temperature. This resulted in the precipitation of small colourless single crystals amongst amorphous material. X-ray analysis of the single crystals showed them to be of a binuclear complex $[Zn_2(HL^1)_2(DMF)_4]\cdot 2(DMF)$ (**1b-Zn**) which crystallises in the triclinic space group $P\bar{1}$ with half of a complex in the asymmetric unit. Two crystallographically identical five-coordinate Zn(II) centres, 7.10 Å apart, are bound by a carboxylate group from each of the two ligands which bridge between them; the remaining carboxylic acid groups on the third arm of each ligand remain protonated and uncoordinated. The first coordinated carboxylate group binds in a monodentate mode [Zn1–O38 1.943(2) Å] whilst the second group binds in a markedly asymmetric bidentate-chelating mode [Zn1–O78 1.982(2) Å, Zn1–O79 2.448(3) Å]. The remaining two coordination sites on each Zn(II) centre are occupied by DMF ligands [Zn1–O1A 2.013(2) Å, Zn1–O1B 1.999(2) Å]. Considering only the four shorter Zn–O bonds, the Zn(II) cations have distorted tetrahedral coordination geometries. The two bridging ligands $(HL^1)^{2-}$ are in *endo*-tripodal conformations with the uncoordinated carboxylic acid groups donating a hydrogen bond to the unbound oxygen atom of a monodentate carboxylate group of a neighbouring complex [O58···O39 2.704(4) Å].

3.2.3. $[Co_{14}(L^2)_6(OH)_8(HCO_2)_2(DMF)_4(H_2O)_6]\cdot 28(DMF)$ (2-Co) and $[Ni_{14}(L^2)_6(OH)_8(HCO_2)_2(DMF)_4(H_2O)_6]\cdot 24(DMF)$ (2-Ni)

Reaction of **H_3L^1** with $Co(NO_3)_2\cdot 6H_2O$ in DMF for 5 days at 85 °C resulted in formation of a crop of pink rhombic plate-like crystals which X-ray analysis showed to be $[Co_{14}(\mathbf{L2})_6(OH)_8(HCO_2)_2(DMF)_4(H_2O)_6]\cdot 28(DMF)$ (**2-Co**). The analogous reaction of **H_3L^1** with $Ni(NO_3)_2\cdot 6H_2O$ resulted in a mixture of an amorphous green precipitate and small green rhombic crystals which X-ray analysis showed to be an isostructural and isomorphous material $[Ni_{14}(\mathbf{L2})_6(OH)_8(HCO_2)_2(DMF)_4(H_2O)_6]\cdot 24(DMF)$ (**2-Ni**). The complexes crystallise in space group $P\bar{1}$ with an asymmetric unit containing one half of a tetradecanuclear M(II) cluster. The fourteen six-coordinate M(II) cations have distorted octahedral geometries and are arranged in an approximately planar elliptical array (mean deviation from plane 0.662 Å, maximum deviation 1.024 Å) with the cations being bridged by a mixture of μ_3-OH groups, carboxylate oxygen atoms and formate anions (Fig. 2). The coordination spheres of the peripheral M(II) cations are completed by monodentate DMF or water ligands. Three ligands $(L^1)^{3-}$ in tripodal *endo* conformations approach the cluster from above the plane of the elliptic array and three approach from below. Each of the three ligands in the asymmetric unit is bound to either four or five M(II) cations in a different fashion *via* a mixture of monodentate, bridging-monodentate, chelating-bidentate, bridging-bidentate and bridging-tridentate coordination modes which are summarised in Harris notation [31] in Table 1. The three tripodal ligands on one face of the complex are twisted in the same sense as each other whilst the three ligands on the other face are twisted in the opposite sense. The complex includes two bridging-tridentate formate ligands formed from decomposition of DMF during the reaction. The eight μ_3-OH groups all donate intramolecular hydrogen bonds to coordinated oxygen donor

atoms of adjacent carboxylate or DMF ligands. The identity of the hydroxy functional groups in **2-Ni** is confirmed by the presence of electron density peaks associated with the hydrogen atoms; these peaks are not apparent in electron density map of **2-Co** as a consequence of weaker diffraction data (Table 2).

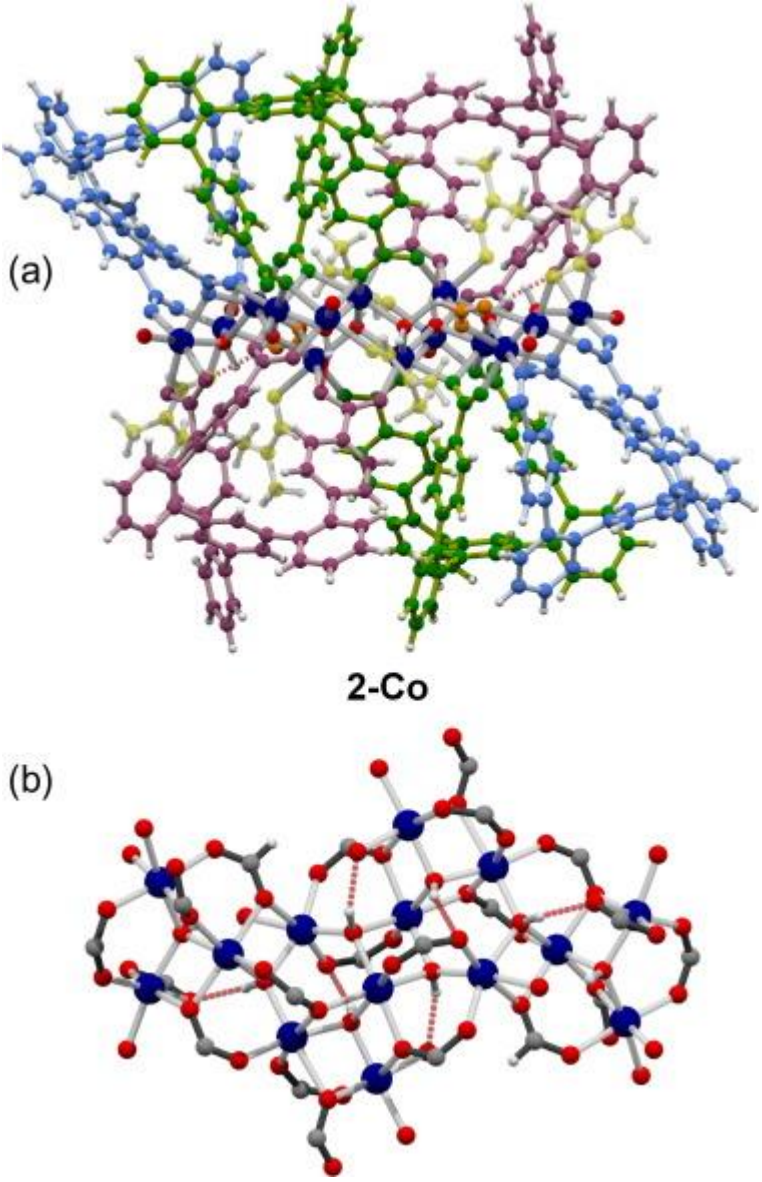

Fig. 2.

View of (a) overall structure and of (b) $Co_{14}(RCO_2)_{18}(\mu_3\text{-}OH)_8(HCO_2)_2$ core in $[Co_{14}(\mathbf{L}^2)_6(\mu_3\text{-}OH)_8(HCO_2)_2(DMF)_4(H_2O)_6]$ (**2-Co**): the three $(\mathbf{L}_1)^{3-}$ ligands are coloured blue, green and purple; DMF yellow; formate orange; cobalt dark blue; oxygen red; intramolecular hydrogen bonds shown as dashed red lines. (Color online.)

Figure options

Table 1.

Selected torsion angles, intramolecular distances, conformations and binding modes for complexes of $\mathbf{H_3L}^{1-4}$.

		Torsion angles [°]				Distances [Å]			
		ϕ^1range	ϕ^1average	$\phi^{2/3}$range	$\phi^{2/3}$average	***d***range	***d***average	Conformation and mode	Harris notation
1a-Zn	$[Zn_8(\mu_4\text{-}O)(\mathbf{L}^1)_4(HCO_2)_2(H_2O)_{0.33}(DMF)_2]\cdot 7.75(DMF)$	46.5–66.1	59.8	42.1–69.5	57.7	5.02–5.45	5.18	endo μ_6	$6.1_1 1_2 1_3 1_4 1_5 1_6$
1b-Zn	$[Zn_2(\mathbf{HL}^1)_2(DMF)_4]\cdot 2(DMF)$	48.9–57.9	53.8	44.6–55.1	50.7	6.27–6.47	6.38	exo μ_2	$2.1_1 1_2 1_2$
2-Co	$[Co_{14}(\mathbf{L}^2)_6(\mu_3\text{-}OH)_8(HCO_2)_2(DMF)_4(H_2O)_6]\cdot 28(DMF)$	46.9–103.5	65.5	30.3–57.4	42.8	3.79–6.31	4.93	endo μ_5 endo μ_5 endo μ_4	$5.1_1 1_1 1_2 1_3 1_4 1_5$ $5.1_1 2_{23} 2_{24} 2_{34} 1_5$ $4.1_1 1_{23} 2_{24} 1_3 1_4$
2-Ni	$[Ni_{14}(\mathbf{L}^2)_6(\mu_3\text{-}OH)_8(HCO_2)_2(DMF)_4(H_2O)_6]\cdot 24(DMF)$	48.2–102.3	66.8	36.5–59.0	46.0	3.84–6.30	5.13	endo μ_5 endo μ_5 endo μ_4	$5.1_1 1_1 1_2 1_3 1_4 1_5$ $5.1_1 2_{23} 2_{24} 2_{34} 1_5$ $4.1_1 1_{23} 2_{24} 1_3 1_4$
3-Zn	$[Zn_8(\mu_4\text{-}O)(\mathbf{L}^3)_4(DMF)(H_2O)_4](NO_3)_2\cdot 16(DMF)$	61.2–69.3	67.6	46.1-58.5	54.3	5.14–5.26	5.19	endo μ_6	$6.1_1 1_2 1_3 1_4 1_5 1_6$
4-Zn	$\{[Zn_3(\mathbf{L}^2)_2(DMF)(H_2O)(C_5H_5N)]\cdot 6(DMF)\}_n$	40.6–56.8	49.0	25.4–59.7	49.0	3.41–7.93	3.44/7.60	exo μ_4	$4.1_1 1_2 1_3 1_4 1_3 1_4$
5-Ni	$[Ni_5(\mu\text{-}OH)_4(\mathbf{L}^2)_2(H_2O)_6(DMF)_4]\cdot 6(DMF)$	42.3–88.4	59.3	36.7–83.6	53.7	3.88–6.19	5.40	endo μ_5	$5.1_1 1_2 1_3 1_4 1_3 1_5$
6-Co	$[Co_8(\mu_4\text{-}O)_4(\mathbf{L}^4)_4(DMF)_3(H_2O)]\cdot 3(H_2O)\cdot 6(DMF)$	40.9–45.9	43.6	44.2–55.8	50.2	4.07–4.23	4.15	endo μ_4	$4.1_1 1_2 1_1 1_3 1_1 1_4$

		Torsion angles [°]				Distances [Å]			
		ϕ^1range	ϕ^1average	$\phi^{2/3}$range	$\phi^{2/3}$average	***d***range	***d***average	Conformation and mode	Harris notation
7-Fe	$[Fe_3(\mu_3\text{-}O)(\mathbf{L}^4)_2(H_2O)(DMF)_2)]\cdot 10(DMF)$	39.6–50.2	45.7	57.7–73.3	64.4	4.23–4.33	4.29	endo μ_3	$3.1_1 1_2 1_2 1_3 1_3 1_1$

Table options

Table 2.

Experimental information for single crystal X-ray structures.

	1a-Zn	**1b-Zn**	**2-Co**	**2-Ni**	**3-Zn**
Chemical formula	$C_{209}H_{173}N_9O3_8Zn_8$	$C_{108}H_{110}N_4O_{18}Zn_2$	$C_{368}H_{408}Co_{14}N_{32}O_{86}$	$C_{356}H_{380}N_{28}Ni_{14}O_{82}$	$C_{342}H_{382}N_{32}O_{69}Zn_8$
M_r	4001.59	1884.75	7480.26	7184.80	5420.89
T (K)	90	90	90	90	120
Crystal system	tetragonal	triclinic	triclinic	triclinic	trigonal
Space group	$I4_1/a$	$P\bar{1}$	$P\bar{1}$	$P\bar{1}$	$R3$
a (Å)	44.7465 (8)	10.0073 (7	18.2047 (12	18.5540 (4	31.3629 (5
b (Å)	44.7465 (8	13.7375 (6	22.9068 (13	22.8380 (5	31.3629 (5)
c (Å)	37.5201 (14)	19.2412 (9)	24.0347 (13)	23.8366 (4)	26.5627 (4)
α (°)	90	72.604 (4)	109.198 (5)	108.7451 (17)	90
β (°)	90	75.194 (5)	97.386 (5)	98.4091 (16)	90
γ (°)	90	75.943 (5)	107.639 (5)	107.482 (2)	120
V (Å^3)	75 125 (4)	2400.3 (2)	8725.6 (10)	8787.1 (3)	22 627.5 (7)
Z (Z')	16 (1)	1 (0.5)	1 (0.5)	1 (0.5)	3 (0.333)
Radiation type	Cu Kα	Cu Kα	Cu Kα	Cu Kα	Cu Kα
μ (mm^{-1})	1.77	1.19	5.78	1.46	1.26

	1a-Zn	1b-Zn	2-Co	2-Ni	3-Zn
Crystal size (mm)	0.37 × 0.11 × 0.03	0.30 × 0.10 × 0.05	0.35 × 0.17 × 0.03	0.28 × 0.19 × 0.05	0.34 × 0.29 × 0.17
Reflections collected	76 065	9407	32 507	79 309	64 262
Independent reflections	34 810	9407	15 195	32 464	20 491
Reflections [$I > 2\sigma(I)$]	14 121	8287	6981	21 310	18 751
R_{int}	0.107	–	0.159	0.049	0.022
$\theta_{maximum}$ (°)	71.8	74.7	47.2	71.3	76.9
$(\sin \theta/\lambda)_{maximum}$ ($Å^{-1}$)	0.616	0.626	0.476	0.614	0.632
$R[F^2 > 2\sigma(F^2)]$	0.086	0.057	0.173	0.061	0.053
$wR(F^2)$ [all data]	0.292	0.144	0.453	0.183	0.159
Goodness-of-fit (GOF) on F^2	0.97	1.11	1.24	1.04	1.03
No. of reflections	34 810	9407	15 195	32 464	20 491
No. of parameters	2124	565	1389	1719	920
No. of restraints	5362	0	2996	2184	856
Largest diff. Peak/hole (e $Å^{-3}$)	0.74, −0.90	0.70, −0.63	1.18, −0.94	1.24, −0.50	1.10, −0.40
CCDC number	1470101	1470096	1470098	1470104	1470099

	4-Zn	5-Ni	6-Co	7-Fe
Chemical formula	$C_{71}H_{65}N_5O_{17}Zn_3$	$C_{102}H_{158}N_{16}Ni_5O_{38}$	$C_{297}H_{383}Co_8N_{39}O_{68}$	$C_{126}H_{140}Fe_3N_{12}O_{26}$
M_r	1675.67	1889.19	3489.38	2341.78
T (K)	90	150	120	120

Crystal system	triclinic	triclinic	trigonal	monoclinic
Space group	$P\bar{1}$	$P\bar{1}$	$P\bar{3}$c1	*P*2/*c*
a (Å)	10.400 (12)	14.8417 (5)	21.658 (3)	27.1936 (14)
b (Å)	20.06 (3)	15.7060 (4)	21.658 (3)	10.9124 (7)
c (Å)	20.73 (3)	21.3256 (6)	44.608 (6)	36.7627 (19)
α (°)	112.33 (3)	90.733 (2)	90	90
β (°)	91.561 (11)	104.580 (3)	90	90
γ (°)	99.563 (19)	100.444 (2)	120	90
V (Å^3)	3927 (9)	4722.4 (2)	18 120 (6)	10564.9 (10)
Z (*Z*′)	2 (1)	2 (0.5)	4 (0.333)	4 (1)
Radiation type	Synchrotron *λ* = 0.6889 Å	Synchrotron *λ* = 0.6889 Å	Cu Kα	Synchrotron *λ* = 0.6889 Å
μ (mm^{-1})	0.99	0.97	6.18	0.49
Crystal size (mm)	0.2 × 0.2 × 0.2	0.05 × 0.02 × 0.02	0.05 × 0.05 × 0.03	0.05 × 0.03 × 0.01
Reflections collected	24 631	61 728	45 639	12 858
Independent reflections	8143	31 529	10 244	12 858
Reflections [$I > 2\sigma(I)$]	6127	22 545	2121	8045
R_{int}	0.082	0.030	0.375	–
$\theta_{maximum}$ (°)	20.8	32.1	74.4	21.3
$(\sin \theta/\lambda)_{maximum}$(Å^{-1})	0.500	0.772	0.625	0.526
R [$F^2 > 2\sigma(F^2)$]	0.121	0.099	0.143	0.142
wR(F^2) [all data]	0.393	0.282	0.458	0.403
Goodness-of-fit (GOF) on F^2	1.52	1.06	0.96	1.33

No. of reflections	8143	31 529	10 244	12 858
No. of parameters	823	1233	684	1036
No. of restraints	2224	2269	868	1961
Largest diff. Peak/hole (e Å^{-3})	1.22, −1.20	2.17, −2.09	0.64, −0.51	1.56, −0.78
CCDC number	1470097	1470102	1470100	1470103

Table options

2-Co was found to be sparingly soluble in CD_3CN allowing the solution behaviour of the complex to be probed by ^1H NMR spectroscopy. The spectrum is dominated by large solvent peaks for DMF, H_2O and diethyl ether alongside which are broad peaks between 1.30 and 3.60 ppm indicating seven proton environments. The number of environments is consistent with the ligands remaining in an approximately C_3 symmetric environment observed in **2-Co** whilst their upfield shifts with respect to uncoordinated ligand **H$_3$L^1**dissolved in d_6-DMSO are consistent with the ligand being complexed to paramagnetic Co(II) [32].

3.2.4. [Zn$_8$(μ$_4$-O)(L^3)$_4$(DMF)(H$_2$O)$_4$](NO$_3$)$_2$·16(DMF) (3-Zn)

Reaction of elongated ligand **H$_3$L^3** with $Zn(NO_3)_2·6H_2O$ in DMF for 3 days at 85 °C resulted in formation of a crop of colourless hexagonal platy crystals which X-ray analysis showed to be $[Zn_8(\mu_4\text{-}O)(\mathbf{L}^3)_4(DMF)(H_2O)_4](NO_3)_2·16(DMF)$ (**3-Zn**), an analogous octanuclear cluster to **1a-Zn** obtained using ligand **H$_3$L^1** (Fig. 1). The complex crystallises in the trigonal space group *R*3 and contains a third of an octanuclear cluster in the asymmetric unit. Although only one enantiomer of the chiral complex appears in the refinement model, the structure is a racemic twin with a twin fraction of 0.52(2). The $[Zn_8O(\mathbf{L3})_4]$ core of the cluster has the same topology as **1a-Zn** with four tripodal ligands in *endo* conformations each spanning three of the four three-blade $[Zn_2(RCO_2)_3]$ paddlewheels. The identity of the anions which balance the +2 charge of the octanuclear core is ambiguous: coordinated ligands at the axial positions three of the Zn(II) centres are modelled as a disordered mixture of DMF and water whilst three disordered water ligands are coordinated at the fourth Zn(II) centre. An electron density peak (1.10 e Å^{-3}) close to the three coordinated water molecules suggests that the missing counter-ion may be a disordered bidentate-chelating nitrate anion but no viable refinement model could be developed.

Despite the elongation of the three arms in **H$_3$L^3** compared with **H$_3$L^1**, similar geometries of the Zn_8O cores in **1a-Zn** and **3-Zn** demand the intramolecular carboxylate-carboxylate distances *d* in the complexed ligands to have similar values (average distances 5.18 and 5.19 Å in **1a-Zn** and **3-Zn**, respectively). The longer arms of **(L3)**$^{3-}$ compared to **(L1)**$^{3-}$result in a steeper average pitch of the propeller twist as observed by comparing the average *ortho*-diphenybenzene torsion angles ϕ^1 in the two structures (59.8° and 67.6° for **1a-Zn** and **3-Zn**, respectively).

3.2.5. {[$Zn_3(L^2)_2(DMF)(H_2O)(C_5H_5N)$]·6(DMF)}$_n$ (4-Zn)

Reaction of the shorter ligand **H_3L^2** with $Zn(NO_3)_2 \cdot 6H_2O$ in DMF and a small amount of pyridine for 3 days at 85 °C resulted in formation of colourless blocky crystals which X-ray analysis showed to be a 2D-coordination network {[Zn_3(**L^2**)$_2$(DMF)(H_2O)(C_5H_5N)]·6(DMF)}$_n$ (**4-Zn**). The network crystallises in space group $P\bar{1}$ and contains three Zn(II) centres and two ligands $(L^2)^{3-}$ in the asymmetric unit, with both ligands in *exo*conformations. The structure is a (4,4)-net consisting of four-bladed paddlewheels {$Zn_2(RCO_2)_4 \cdot (solv)_2$} acting as four-connected nodes and ligands (**L2**)$^{3-}$ acting as linkers (Fig. 3). Each ligand in the asymmetric unit coordinates via two carboxylate groups to adjacent Zn(II) sites of a single paddlewheel and a third carboxylate group is coordinated to a different paddlewheel. Of the three types of paddlewheel in the asymmetric unit, two are coordinated at adjacent sites by pairs of carboxylate groups from two ligands, thus topologically making them linkers, whilst the third type of paddlewheel is coordinated by carboxylate groups from four different ligands, making it a four-connected node. The axial Zn(II) coordination sites of the four-connected paddlewheel units are occupied by pyridyl ligands, with the axial coordination sites of the linking paddlewheels occupied by DMF and water ligands. The centroid–centroid distances between the four-connected nodes along the edges of the (4,4) net are 21.0 and 20.7 Å and the internal angles of the net are 112.1° and 67.2°. The (4,4) nets are stacked directly on top of each other resulting in narrow pores containing disordered solvent running through the holes in the nets.

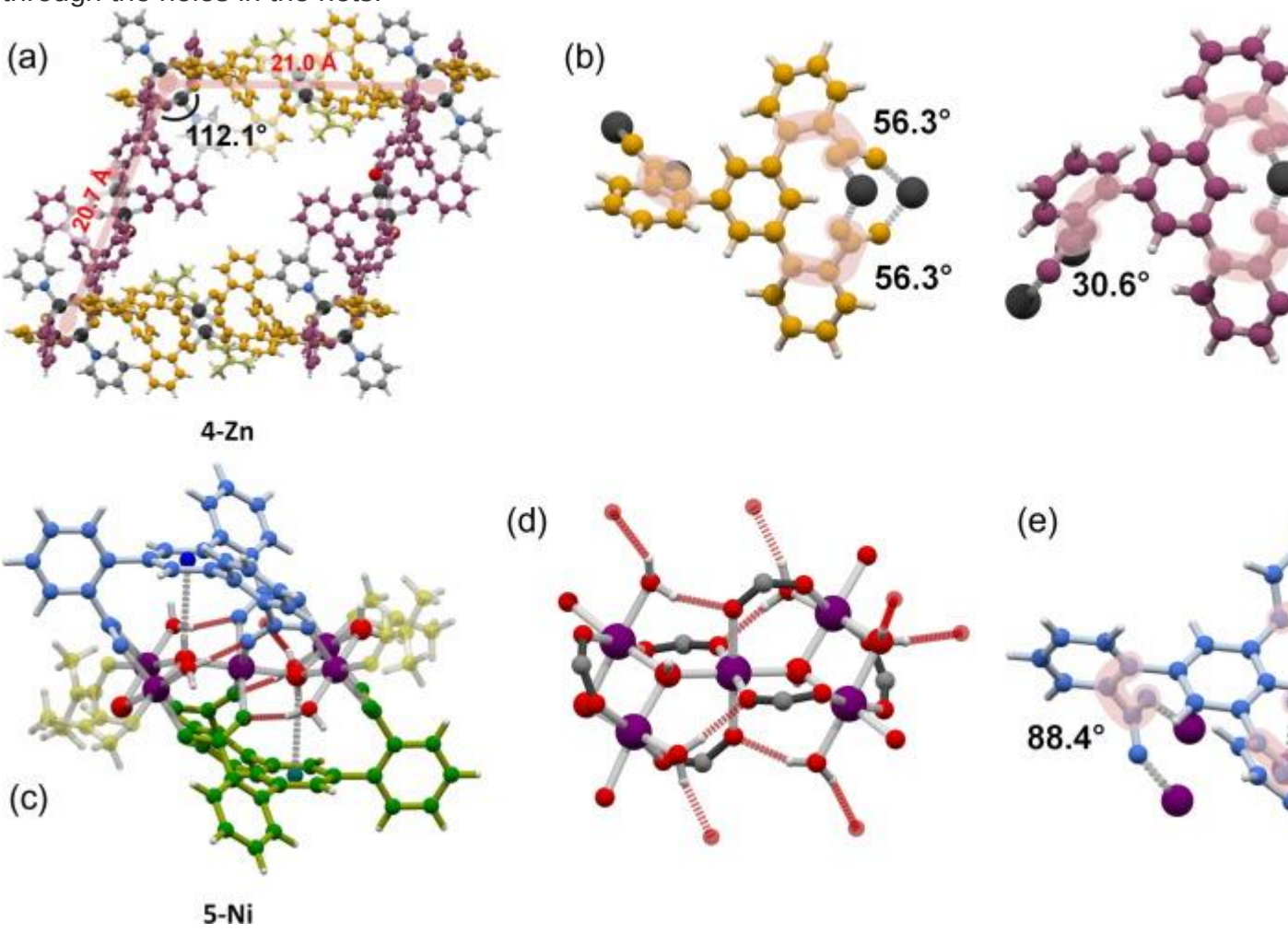

Fig. 3.

View of (a) structure of {[Zn_3(**L**^{2})$_2$(DMF)(H_2O)(C_5H_5N)] (**4-Zn**) showing one repeat unit of the (4,4)-net highlighting the inter-node distances and angles: the ligands (**L2**)$^{3-}$ are coloured yellow and purple; DMF yellow; pyridine grey; zinc black; oxygen red. (b) View of conformations and coordination environments of the two ligands in the asymmetric unit of **4-Zn** with phenyl-carboxylate torsion angles ϕ^3 highlighted. View of (c) overall structure and of (d) Ni_5(μ-OH)$_4$(RCO_2)$_6$(H_2O)$_6$ core in [Ni_5(μ-OH)$_4$(**L**^{2})$_2$(H_2O)$_6$(DMF)$_4$] (**5-Ni**): ligands are coloured blue, green; DMF yellow; nickel purple; oxygen red; hydrogen bonds red dashed lines; O–H···phenyl face interactions grey dashed lines. (e) Conformations and coordination environments of one ligand from **5-Ni** with phenyl-carboxylate torsion angles ϕ^3 highlighted. (Color online.)

Figure options

The ability of ligand (**L2**)$^{3-}$ to coordinate at adjacent positions of a Zn(II) paddlewheel is permitted by the 90° bite angle between the carboxylate groups in the 1,3-*bis*-carboxyphenylbenzene unit, a motif previously seen in a W-shaped tetracarboxylic acid ligand described by Zhang [33]. In **4-Zn** the twist between the carboxylate groups and phenyl rings described by torsion angle ϕ^3 (range 25.4–59.7°) indicates unusually large deviations from planarity which are necessary to align the plane of the carboxylate groups with the Zn-Zn axis of the paddlewheel moiety.

3.2.6. [Ni_5(μ-OH)$_4$(L^2)$_2$(H_2O)$_6$(DMF)$_4$]·6(DMF) (5-Ni)

Reaction of **H_3L**^{2} with $Ni(NO_3)_2$·$6H_2O$ in DMF for 5 days at 80 °C did not result in the formation of a precipitate. Diisopropyl ether was diffused into the resulting green solution leading to formation of a small number of green block-like crystals which were shown by X-ray analysis to be [Ni_5(μ-OH)$_4$(**L**^{2})$_2$(H_2O)$_6$(DMF)$_4$]·6(DMF) (**5-Ni**). The asymmetric unit in space group $P\bar{1}$ contains one pentanuclear cluster.

The five six-coordinate Ni(II) cations have distorted octahedral geometries and lie in a plane (mean deviation from plane 0.002 Å) arranged as two isosceles triangles with a shared vertex (short edge average Ni···Ni distance 2.98 Å, long edge average Ni···Ni distance 3.60 Å). A $μ_3$-OH group is found at the centre of each Ni_3 triangle whilst a $μ_2$-OH bridges two Ni(II) centres along the short edge of each triangle. The two $μ_3$-OH groups direct their hydrogen atoms towards the central phenyl rings of each ligand (H···ring centroid distances 2.97 and 2.98 Å). A ligand (**L2**)$^{3-}$ straddles each face of the pentanuclear array with all six carboxylate functional groups spanning two Ni(II) cations in bidentate-bridging modes. The two ligands (**L2**)$^{3-}$ adopt identical *endo* conformations with approximate C_S symmetry in contrast to the C_3 symmetry exhibited by the other ligands with tripodal *endo* conformations described in this work. Two of the carboxylate groups on each ligand are oriented towards each other allowing them to bridge between Ni(II) cations in the same triangular Ni_3 array. The third arm of each ligand and its pendant carboxylate group adopt highly unusual near-perpendicular twists as described by torsion angles ϕ^1 (82.8° and 84.5°) and ϕ^3 (84.2° and 84.1°) which enable the carboxylate groups to bridge the two Ni(II) cations at each end of the structure. Torsion angles so close to 90° in these situations are rare: a search of the CSD [34] ; [35] using Mogul [36] returns no other examples of transition metal bound phenylcarboxylates with torsion angles greater than 80°; the next highest value reported is 78.8° in a coordination framework containing Zn(II) and benzene-1,3,5-tricarboxylic acid [37].

3.2.7. [Co_8($μ_4$-O)$_4$(L4)$_4$(DMF)$_3$(H_2O)]·3(H_2O)·6(DMF) (6-Co)

Reaction of ligand **H_3L**^{4} with $Co(NO_3)_2$·$6H_2O$ in DMF for 2 days at 80 °C resulted in formation of black block crystals which were shown by X-ray analysis to be [Co_8($μ_4$-O)$_4$(**L4**)$_4$(DMF)$_3$(H_2O)]·3(H_2O)·6(DMF) (**6-Co**). The octanuclear cluster crystallises in

the trigonal space group $P\bar{3}c1$ with one third of the complex in the asymmetric unit. Four ligands ($\mathbf{L4}$)$^{3-}$ in tripodal *endo* conformations surround a Co_4O_4 cubane core (Fig. 4) in which four vertices are occupied by six-coordinate Co(III) cations with distorted octahedral geometries whilst the other four vertices are occupied by μ_4-O oxo anions (average Co–O bond length along cube edges 1.90 Å). Each of the four μ_4-O cube corners is coordinated to a peripheral five-coordinate Co(II) cation with distorted trigonal bipyramidal geometry resulting in a Co_8O_4 core isostructural with a cluster containing mono-functional benzoate ligands reported by Christou et al. [38]. The carboxylate groups of all four ligands coordinate in a bidentate-bridging fashion with three of their oxygen atoms chelated to the same central Co(III) cation and the other oxygen atom of each carboxylate coordinated to a peripheral Co(II) cation. This *tris*-chelating coordination mode is made possible by the *meta*-substitution pattern of the carboxylic acid functional groups in $\mathbf{H_3L^4}$ in contrast to the *para*-substitution found in $\mathbf{H_3L^1}$ and $\mathbf{H_3L^3}$.This geometry means that in **6-Co**, despite ligand ($\mathbf{L4}$)$^{3-}$ having a shallow propeller pitch (described by an average torsion angle ϕ^1 of 43.6°), the intra-ligand distances *d* between the carboxylate carbon atoms are very short with an average value of 4.15 Å. Each *meta*-substituted phenyl ring of the ligands ($\mathbf{L4}$)$^{3-}$ within **6-Co** is involved in an aromatic π–π stacking interaction with the equivalent ring of a neighbouring ligand (ring centroid–centroid distance 4.62 and 4.29 Å, centroid-ring mean plane distance 3.72 and 3.90 Å) with a total of six such interactions occurring across the complex. The assignment of the oxidation states of the cobalt atoms is confirmed by bond-valence sum analysis [39] ; [40]indicating an average valence of +3.12 for the inner six-coordinate cations and an average valence of +2.01 for the outer five-coordinate cations. The requirement for atmospheric O_2 to oxidise the Co(II) starting material during formation of the mixed valence species **6-Co** was confirmed by an attempted reaction in oxygen-free conditions: no precipitate was formed even after heating the reaction mixture at 80 °C for 5 days.

(a)

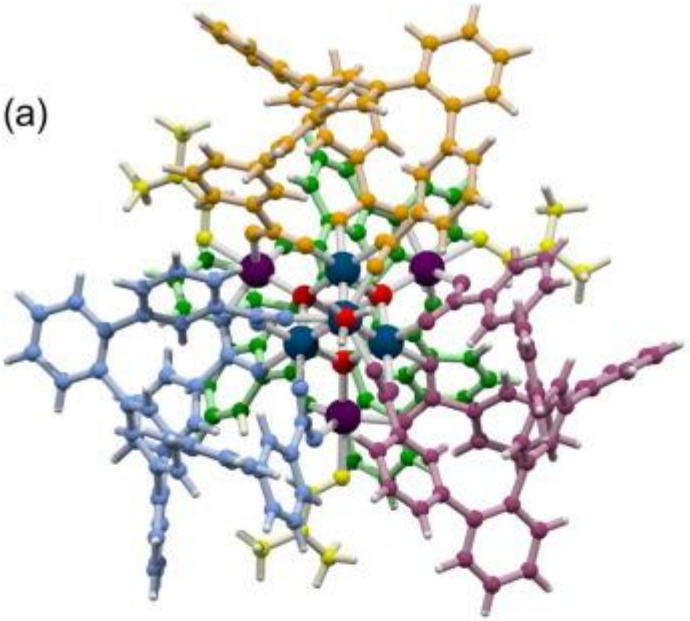

6-Co

(b)

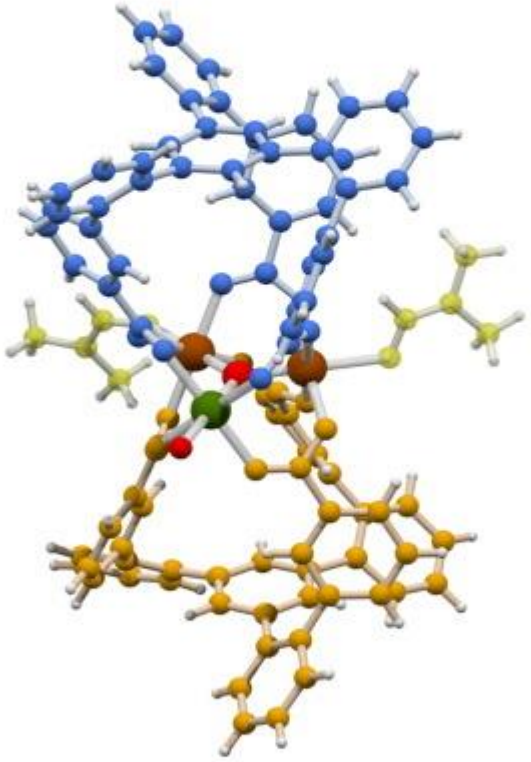

7-Fe

(c)

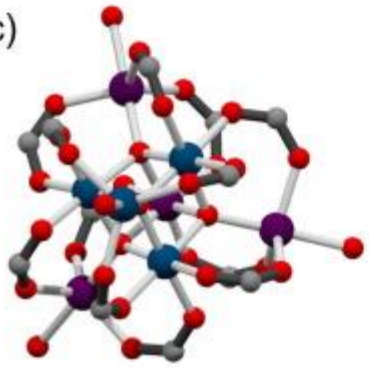

(d)

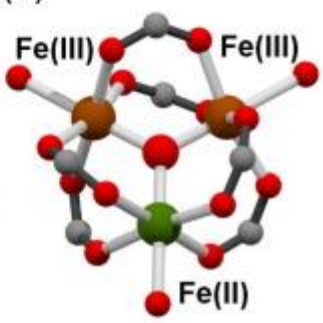

Fig. 4.

View of (a) overall structure and (c) $Co_8(\mu_4\text{-}O)_4(RCO_2)_{12}$ core in $[Co_8(\mu_4\text{-}O)_4(\mathbf{L}^4)_4(DMF)_3(H_2O)]$ (**6-Co**): ligands are coloured orange, blue, purple and green; DMF yellow; cobalt (III) dark teal; cobalt(II) purple; oxygen red. View of (b) overall structure and (d) $Fe_3(\mu_3\text{-}O)(RCO_2)_6$ core in $[Fe_3(\mu^3\text{-}O)(\mathbf{L}^4)_2(H_2O)(DMF)_2)]$ (**7-Fe**): ligands are coloured blue and orange; DMF yellow; iron(II) green; iron(III) brown; oxygen red. (Color online.)

Figure options

The molecular packing in the structure of **6-Co** features alternating offset trigonal layers of clusters resulting in a hexagonal close-packed arrangement of the roughly spherical species (Fig. S4). The packing leaves large intermolecular cavities connected by small hexagonal channels running parallel to the *c*-axis. The total fraction of potential void space in the structure after removal of all non-coordinated solvent and exchange of coordinated DMF for water is calculated as 30.6% by PLATON [41] using a 1.20 Å probe after input of a manually modified structure file. A bulk sample of **6-Co** was solvent-exchanged with acetone and dried in air before a PXRD pattern was measured. The pattern indicated retention of crystallinity and was indexed to give a unit cell showing good agreement with that of the single crystal X-ray structure (Fig. S5). The observation that this large supramolecular complex is stable to solvent exchange and solvent loss is explained by the large numbers of weak intermolecular aromatic π-π stacking and edge-face interactions. Each cluster makes in total six stacking interactions and three edge-face interactions with its six neighbours, giving a total of nine stabilising contacts per molecule.

3.2.8. $Fe_3(\mu_3\text{-}O)(L^4)_2(H_2O)(DMF)_2)]\cdot 10(DMF)$ (7-Fe)

Reaction of ligand $\mathbf{H_3L}^4$ with $Fe(NO_3)_3\cdot nH_2O$ (n = 6–9) in DMF for 2 days at 80 °C resulted in formation of small brown crystals amongst an amorphous precipitate. Single crystals taken directly from the mixture were shown by X-ray analysis to be $[Fe_3(\mu_3\text{-}O)(\mathbf{L4})_2(H_2O)(DMF)_2)]\cdot 10(DMF)$ (**7-Fe**). The trinuclear cluster crystallises in the monoclinic space group *P*2/*c* with one complete complex in the asymmetric unit. The core of the cluster adopts the common $[Fe_3O(RCO_2)_6]$ basic carboxylate motif previously seen in both discrete complexes [42] ; [43] and as a 6-connected connectors in MOFs [44] ; [45]. Three iron centres in an isosceles triangular array (Fe···Fe distances 3.262(3), 3.338(2) and 3.339(2) Å) surround a central μ_3-O with which they are approximately co-planar (mean deviation from Fe_3O plane 0.006 Å). The iron centres are all 6-coordinate and have distorted octahedral geometries comprising four carboxylate oxygen atoms from different groups, the oxo oxygen atom and a neutral water molecule or DMF oxygen atom. A ligand $(\mathbf{L4})^{3-}$ in a tripodal *endo* conformation caps each side of the triangular array, with the edges of the triangle bridged by a carboxylate group from each ligand. Both tripodal ligands are twisted in the same sense, resulting in a chiral complex, but the structure is a racemic mixture [twin fraction 0.279(6)] with complexes of both chiralities represented in the unit cell. Bond-valence sum analysis [39] ; [40] of the three iron centres leads to the identification of mixed oxidation states with Fe1 (BVS sum + 2.92) and Fe2 (BVS sum + 2.89) being assigned as Fe(III) and Fe3 (BVS sum + 2.12) being assigned as Fe(II). The mixed oxidation state arrangement results in **7-Fe** being a charge-balanced neutral complex, but the absence of an associated counterion in the structure cannot be used to support the assignment owing to the disorder in the remainder of the unit cell. The structure of **7-Fe** permits a clear view of the influence of the mixed oxidation states on the bond lengths and geometries of the Fe_3O core; in many reported examples of mixed oxidation state cores the clusters are located on crystallographic special positions, thereby obscuring the

important deviations from perfect threefold symmetry by showing only average atomic positions [46]. This is only the third example in the Cambridge Structural Database of a ligand able to bind in a bridging mode between multiple coordination positions of an $[M_3O(RCO_2)_6]$ cluster [47] ; [48] and the first example of a ligand able to bridge three positions. The stabilisation conferred upon the complex by the match between the ligand and cluster geometries offers enhanced opportunities to investigate and exploit the rich electrochemistry and magnetochemistry of this motif in its roles as an SBU [45], enzyme mimic [48] and catalyst [49].

4. Conclusions

The family of *tris*-carboxylic acid ligands **$H_3L^{1–4}$** reported herein has built upon the earlier promise of **H_3L^1** by acting as tripodal polytopic ligands to form a wide variety of polynuclear metallo-clusters when complexed with the first-row transition metal centres Fe(II/III), Co(II/III), Ni(II), Cu(II) and Zn(II). The threefold symmetric ligands share a common *ortho*-substitution pattern in the attachment of their three arms to a central 1,3,5-substituted phenyl core. This motif has shown itself to be a versatile tool for the construction of polynuclear clusters, allowing the ligands to position their three carboxylic acid binding sites in close proximity to each other. The distance *d* between the binding sites in the semi-rigid ligands is seen to vary to match the geometric demands of the cluster, with carboxylate carbon–carbon separations varying between 3.84 and 7.93 Å across the nine transition metal complex structures described.

Reaction of ligand **H_3L^1** with $Zn(NO_3)_2{\cdot}6H_2O$ at 85 °C resulted in formation of an oxo-centred octanuclear cluster $[Zn_8(\mu_4\text{-}O)(\mathbf{L_1})_4(HCO_2)_2(H_2O)_{0.33}(DMF)_2]{\cdot}7.75(DMF)$ (**1a-Zn**) with four ligands $(\mathbf{L_1})^{3-}$ each coordinated to a three-blade $\{Zn_2(RCO_2)_3\}$ paddlewheel. Reaction of the same metal and ligand at ambient temperature resulted in a different binuclear complex $[Zn_2(\mathbf{HL^1})_2(DMF)_4]{\cdot}2(DMF)$ (**1b-Zn**) containing coordinatively unsaturated ligands $(\mathbf{HL^1})^{2-}$. Reaction of extended ligand **H_3L^3** with $Zn(NO_3)_2{\cdot}6H_2O$ at 85 °C resulted in formation of an isostructural octanuclear cluster $[Zn_8(\mu_4\text{-}O)(\mathbf{L_3})_4(DMF)(H_2O)_4](NO_3)_2{\cdot}16(DMF)$ (**3-Zn**) and demonstrated the ability of the longer ligand to adjust to the stereochemical requirements of the Zn_8O core. Reaction of the shorter ligand **H_3L^2** with $Zn(NO_3)_2{\cdot}6H_2O$ at 85 °C resulted in formation of a 2D-coordination network $\{[Zn_3(\mathbf{L^2})_2(DMF)(H_2O)(C_5H_5N)]{\cdot}6(DMF)\}_n$ with $(L^2)^{3-}$ in an *endo*conformation as a result of the ligand being able to coordinate to two adjacent sites of a $\{Zn_2(CO_2R)_2\}$ four-blade paddle SBU[22].

Reaction of ligand **H_3L^1** with $Co(NO_3)_2{\cdot}6H_2O$ and $Ni(NO_3)_2{\cdot}6H_2O$ at 85 °C resulted in formation of isostructural polynuclear clusters $[Co_{14}(\mathbf{L^2})_6(\mu_3\text{-}OH)_8(HCO_2)_2(DMF)_4(H_2O)_6]{\cdot}28(DMF)$ (**2-Co**) and $[Ni_{14}(\mathbf{L^2})_6(\mu_3\text{-}OH)_8(HCO_2)_2(DMF)_4(H_2O)_6]{\cdot}24(DMF)$ (**2-Ni**) in which six ligands in *endo* conformations act in multiple bridging modes between M(II) cations. The differing conformations of the ligands in these complexes allow them to saturate all the M(II) coordination sites of the low symmetry clusters. Reaction of the shorter ligand **H_3L^2** with $Ni(NO_3)_2{\cdot}6H_2O$ at 85 °C resulted in formation of a pentanuclear cluster $[Ni_5(\mu\text{-}OH)_4(\mathbf{L^2})_2(H_2O)_6(DMF)_4]{\cdot}6(DMF)$ (**Ni-5**) where the ligands $(\mathbf{L_2})^{3-}$ are in *endo* conformations with approximate $C_s$symmetries. The stereochemical requirements of the Ni_5 core results in both ligands exhibiting unprecedented torsion angles close to perpendicular between the central phenyl ring and phenylcarboxylate arm (ϕ^1, 82.8° and 84.5°), and also between the phenylcarboxylate ring and carboxylate functional group (ϕ^3, 84.2° and 84.1°).

Reaction of *meta*-substituted ligand **H_3L^4** with $Co(NO_3)_2 \cdot 6H_2O$ at 80 °C resulted in formation of a mixed oxidation state octanuclear cluster $[Co_8(\mu_4\text{-}O)_4(\mathbf{L4})_4(DMF)_3(H_2O)] \cdot 3(H_2O) \cdot 6(DMF)$ (**6-Co**) in which four ligands $(\mathbf{L4})^{3-}$ in *endo*conformations surround a $Co(III)_4O_4$ cubane core. The *meta*-substitution pattern of ligand **H_3L^4** makes it possible for the three carboxylate groups to adopt the *tris*-chelating mode necessary to coordinate to the compact cluster. The potentially porous bulk material features multiple intramolecular aromatic stacking and edge-face interactions and retained its crystallinity and packing structure upon solvent exchange with acetone. Reaction of the same *meta*-substituted ligand **H_3L^4** with $Fe(NO_3)_3 \cdot nH_2O$ at 80 °C resulted in formation of a trinuclear cluster $[Fe_3(\mu_3\text{-}O)(\mathbf{L4})_2(H_2O)(DMF)_2)] \cdot 10(DMF)$ (**7-Fe**) in which a ligand caps each triangular face of the Fe_3O core. The iron centres in the cluster have mixed oxidation states with two Fe(III) cations and one Fe(II) cation resulting in a charge-neutral complex. This is the first example of a tritopic ligand able to cap the faces of the ubiquitous basic carboxylate M_3O species leading to the possibility stabilising a wider variety of these widely studied motifs.

Acknowledgements

We thank EPSRC UK (award numbers EP/K038869, EP/I011870), ERC (ERC-2008-AdG 226593 to MS) and General Motors for funding. NRC acknowledges the receipt of a Royal Society Wolfson Merit Award. We thank Sihai Yang for help collecting synchrotron PXRD data.

Appendix A. Supplementary data

Supplementary data.

Help with DOCX files

Options

References

1.
- [1]
- R.A. Bilbeisi, J.-C. Olsen, L.J. Charbonnière, A. Trabolsi
- Inorg. Chim. Acta, 417 (2014), p. 79
- Article | PDF (9885 K) | View Record in Scopus | Citing articles (20)

2.
- [2]
- N. Ahmad, H.A. Younus, A.H. Chughtai, F. Verpoort

- Chem. Soc. Rev., 44 (2015), p. 9
- CrossRef | View Record in Scopus | Citing articles (71)

3. [3]
   - M.A. Palacios, E. Moreno Pineda, S. Sanz, R. Inglis, M.B. Pitak, S.J. Coles, M. Evangelisti, H. Nojiri, C. Heesing, E.K. Brechin, J. Schnack, R.E. Winpenny
   - ChemPhysChem, 17 (2016), p. 55
   - CrossRef | View Record in Scopus | Citing articles (6)
4. [4]
   - M.C. Gimenez-Lopez, F. Moro, A. La Torre, C.J. Gomez-Garcia, P.D. Brown, J. van Slageren, A.N. Khlobystov
   - Nat. Commun., 2 (2011), p. 407
5. [5]
   - J.S. Kanady, E.Y. Tsui, M.W. Day, T. Agapie
   - Science, 333 (2011), p. 733
   - CrossRef | View Record in Scopus | Citing articles (251)
6. [6]
   - M.J. Wiester, P.A. Ulmann, C.A. Mirkin
   - Angew. Chem., Int. Ed., 50 (2011), p. 114
   - CrossRef | View Record in Scopus | Citing articles (343)
7. [7]
   - T.R. Cook, Y.R. Zheng, P.J. Stang
   - Chem. Rev., 113 (2013), p. 734

- CrossRef | View Record in Scopus | Citing articles (1198)

8. [8]
   - D. Lee, S.J. Lippard
   - J. Am. Chem. Soc., 120 (1998), p. 12153
   - CrossRef | View Record in Scopus | Citing articles (105)
9. [9]
   - E.C. Carson, S.J. Lippard
   - Inorg. Chem., 45 (2006), p. 837
   - CrossRef | View Record in Scopus | Citing articles (35)
10. [10]
    - N. Taleb, V.J. Richards, S.P. Argent, J. van Slageren, W. Lewis, A.J. Blake, N.R. Champness
    - Dalton Trans., 40 (2011), p. 5891
    - View Record in Scopus | Citing articles (8)
11. [11]
    - T.K. Ronson, H. Nowell, A. Westcott, M.J. Hardie
    - Chem. Commun., 47 (2011), p. 176
    - CrossRef | View Record in Scopus | Citing articles (31)
12. [12]
    - A. Baniodeh, C.E. Anson, A.K. Powell
    - Chem. Sci., 4 (2013), p. 4354

- CrossRef
  |
  View Record in Scopus
  |
  Citing articles (21)

13.
- [13]
- X. Zhang, L. Fan, W. Fan, B. Li, X. Zhao
- CrystEngComm, 17 (2015), p. 6681
- CrossRef
  |
  View Record in Scopus
  |
  Citing articles (15)

14.
- [14]
- C. Tan, S. Yang, N.R. Champness, X. Lin, A.J. Blake, W. Lewis, M. Schröder
- Chem. Commun., 47 (2011), p. 4487
- CrossRef
  |
  View Record in Scopus
  |
  Citing articles (140)

15.
- [15]
- S. Yang, J. Sun, A.J. Ramirez-Cuesta, S.K. Callear, W.I.F. David, D.P. Anderson, R. Newby, A.J. Blake, J.E. Parker, C.C. Tang, M. Schröder
- Nat. Chem., 4 (2012), p. 887
- CrossRef
  |
  View Record in Scopus
  |
  Citing articles (159)

16.
- [16]
- S. Yang, A.J. Ramirez-Cuesta, R. Newby, V. Garcia-Sakai, P. Manuel, S.K. Callear, S.I. Campbell, C.C. Tang, M. Schröder
- Nat. Chem., 7 (2015), p. 121
- CrossRef
  |
  View Record in Scopus
  |
  Citing articles (3)

17.
- [17]
- Y. Yan, S. Yang, A.J. Blake, M. Schröder
- Acc. Chem. Res., 47 (2014), p. 296
- View Record in Scopus | Citing articles (131)

18.
- [18]
- S.P. Argent, A. Greenaway, M.C. Giménez-López, W. Lewis, H. Nowell, A.N. Khlobystov, A.J. Blake, N.R. Champness, M. Schröder
- J. Am. Chem. Soc., 134 (2012), p. 55
- CrossRef | View Record in Scopus | Citing articles (41)

19.
- [19]
- S.M. Mathew, J.T. Engle, C.J. Ziegler, C.S. Hartley
- J. Am. Chem. Soc., 135 (2013), p. 6714
- CrossRef | View Record in Scopus | Citing articles (39)

20.
- [20]
- M.-T. Kao, J.-H. Chen, Y.-Y. Chu, K.-P. Tseng, C.-H. Hsu, K.-T. Wong, C.-W. Chang, C.-P. Hsu, Y.-H. Liu
- Org. Lett., 13 (2011), p. 1714
- CrossRef | View Record in Scopus | Citing articles (16)

1.
- [21]
- H. Noguchi, K. Hojo, M. Suginome
- J. Am. Chem. Soc., 129 (2007), p. 758
- CrossRef | View Record in Scopus |

Citing articles (190)

2.
- [22]
- X. Feng, J. Wu, V. Enkelmann, K. Müllen
- Org. Lett., 8 (2006), p. 1145
- CrossRef | View Record in Scopus | Citing articles (66)

3.
- [23]
- B. Buchanan, M. Collard
- J. Anthropol. Archaeol., 26 (2007), p. 366
- Article | PDF (661 K) | View Record in Scopus | Citing articles (79)

4.
- [24]
- **CrysAlis Pro**
- Agilent Technologies Ltd, Yarnton, Oxfordshire, England (2014)

5.
- [25]
- H. Nowell, S.A. Barnett, K.E. Christensen, S.J. Teat, D.R. Allan
- J. Synchrotron Radiat., 19 (2012), p. 435
- CrossRef | View Record in Scopus | Citing articles (62)

6.
- [26]
- CrystalClear. Rigaku MSC, 491 South Orem Blvd, Orem, UT 84058, USA, 2010.

7.
- [27]
- G. Sheldrick
- Acta Crystallogr. Sect. C, 71 (2015), p. 3
- CrossRef |

View Record in Scopus

|

Citing articles (2376)

8.
- [28]
- G. Pawley
- J. Appl. Crystallogr., 14 (1981), p. 357
- CrossRef

9.
- [29]
- TOPAS-Academic V5. Coelho Software, Brisbane, Australia, 2012.
-

10.
- [30]
- S. Vagin, A.K. Ott, B. Rieger
- Chem. Ing. Tech., 79 (2007), p. 767
- CrossRef

|

View Record in Scopus

|

Citing articles (56)

11.
- [31]
- R.A. Coxall, S.G. Harris, D.K. Henderson, S. Parsons, P.A. Tasker, R.E.P. Winpenny
- J. Chem. Soc., Dalton Trans. (2000), p. 2349
- CrossRef

|

View Record in Scopus

|

Citing articles (364)

12.
- [32]
- R.L. Paul, S.P. Argent, J.C. Jeffery, L.P. Harding, J.M. Lynam, M.D. Ward
- Dalton Trans. (2004), p. 3453
- CrossRef

|

View Record in Scopus

|

Citing articles (82)

13.
- [33]
- L. Fan, W. Fan, B. Li, X. Zhao, X. Zhang
- RSC Adv., 5 (2015), p. 39854
- CrossRef

|

View Record in Scopus

|

Citing articles (11)

14.
- [34]
- C.R. Groom, F.H. Allen
- Angew. Chem., Int. Ed., 53 (2014), p. 662
- CrossRef

|

View Record in Scopus

|

Citing articles (664)

15.
- [35]
- C.R. Groom, I.J. Bruno, M.P. Lightfoot, S.C. Ward
- Acta Crystallogr. B, 72 (2016), p. 171
- CrossRef

|

View Record in Scopus

|

Citing articles (680)

16.
- [36]
- I.J. Bruno, J.C. Cole, M. Kessler, J. Luo, W.D.S. Motherwell, L.H. Purkis, B.R. Smith, R. Taylor, R.I. Cooper, S.E. Harris, A.G. Orpen
- J. Chem. Inf. Comput. Sci., 44 (2004), p. 2133
- CrossRef

|

View Record in Scopus

|

Citing articles (429)

17.
- [37]
- P. Li, J. Lou, Y. Zhou, X. Liu, Z. Chen, L. Weng
- Dalton Trans. (2009), p. 4847
- CrossRef

|

View Record in Scopus

|

Citing articles (13)

18.
- [38]
- K. Dimitrou, J.-S. Sun, K. Folting, G. Christou

- Inorg. Chem., 34 (1995), p. 4160
- CrossRef
  |
  View Record in Scopus
  |
  Citing articles (60)

19.
- [39]
- H.H. Thorp
- Inorg. Chem., 31 (1992), p. 1585
- CrossRef
  |
  View Record in Scopus
  |
  Citing articles (306)

20.
- [40]
- R.M. Wood, K.A. Abboud, R.C. Palenik, G.J. Palenik
- Inorg. Chem., 39 (2000), p. 2065
- CrossRef
  |
  View Record in Scopus
  |
  Citing articles (44)

1.
- [41]
- A. Spek
- Acta Crystallogr. Sect. D, 65 (2009), p. 148
- CrossRef
  |
  View Record in Scopus
  |
  Citing articles (10804)

2.
- [42]
- V.M. Lynch, J.W. Sibert, J.L. Sessler, B.E. Davis
- Acta Crystallogr. Sect. C, 47 (1991), p. 866
- CrossRef
  |
  View Record in Scopus
  |
  Citing articles (24)

3.
- [43]
- A.K. Boudalis, Y. Sanakis, C.P. Raptopoulou, A. Terzis, J.-P. Tuchagues, S.P. Perlepes
- Polyhedron, 24 (2005), p. 1540
- Article | PDF (313 K) | View Record in Scopus | Citing articles (30)

4.
- [44]
- C. Serre, F. Millange, S. Surble, G. Ferey
- Angew. Chem., Int. Ed., 43 (2004), p. 6285
- CrossRef | View Record in Scopus | Citing articles (122)

5.
- [45]
- D. Feng, K. Wang, Z. Wei, Y.P. Chen, C.M. Simon, R.K. Arvapally, R.L. Martin, M. Bosch, T.F. Liu, S. Fordham, D. Yuan, M.A. Omary, M. Haranczyk, B. Smit, H.C. Zhou
- Nat. Commun., 5 (2014), p. 5723
- CrossRef | View Record in Scopus | Citing articles (42)

6.
- [46]
- A.C. Sudik, A.P. Côté, O.M. Yaghi
- Inorg. Chem., 44 (2005), p. 2998
- CrossRef | View Record in Scopus | Citing articles (167)

7.
- [47]
- Y. Li, J.J. Wilson, L.H. Do, U.-P. Apfel, S.J. Lippard
- Dalton Trans., 41 (2012), p. 9272

- CrossRef
  |
  View Record in Scopus
  |
  Citing articles (4)

8.
- [48]
- V. Rabe, W. Frey, A. Baro, S. Laschat, M. Bauer, H. Bertagnolli, S. Rajagopalan, T. Asthalter, E. Roduner, H. Dilger, T. Glaser, D. Schnieders
- Eur. J. Inorg. Chem. (2009), p. 4660
- CrossRef
  |
  View Record in Scopus
  |
  Citing articles (18)

9.
- [49]
- S. Uchida, A. Lesbani, Y. Ogasawara, N. Mizuno
- Inorg. Chem., 51 (2012), p. 775
- CrossRef
  |
  View Record in Scopus
  |
  Citing articles (17)

Corresponding authors at: School of Chemistry, University of Manchester, Oxford Road, Manchester M13 9PL, UK.